HHS Public Access

Author manuscript

ACS Biomater Sci Eng. Author manuscript; available in PMC 2022 October 03.

Published in final edited form as:

ACS Biomater Sci Eng. 2020 October 12; 6(10): 5771–5784. doi:10.1021/acsbiomaterials.0c00844.

Acute implantation of aligned hydrogel tubes supports delayed spinal progenitor implantation

Andrew J. Ciciriello[1,2], **Dominique R. Smith**[3], **Mary K. Munsell**[3], **Sydney J. Boyd**[1], **Lonnie D. Shea**[3,4], **Courtney M. Dumont**[1,2,*]

[1]Department of Biomedical Engineering, University of Miami, 1251 Memorial Drive, Coral Gables, Florida 33156, United States

[2]Biomedical Nanotechnology Institute at the University of Miami (BioNIUM), University of Miami, 1951 NW 7th Avenue Ste. 475, Miami, Florida 33136, United States

[3]Department of Biomedical Engineering, University of Michigan, 2200 Bonisteel Boulevard, Ann Arbor, Michigan 48109, United States

[4]Department of Chemical Engineering, University of Michigan, 2300 Hayward Street, Ann Arbor, Michigan 48109, United States

Abstract

An important role of neural stem cell transplantation is repopulating neural and glial cells that actively promote repair following spinal cord injury (SCI). However, stem cell survival after transplantation is severely hampered by the inflammatory environment that arises after SCI. Biomaterials have a demonstrated history of managing post-SCI inflammation and can serve as a vehicle for stem cell delivery. In this study, we utilize macroporous polyethylene glycol (PEG) tubes, that were previously found to modulate the post-SCI microenvironment, to serve as a viable, soft substrate for injecting mouse embryonic day 14 (E14) spinal progenitors two weeks after tube implantation into a mouse SCI model. At two weeks after transplantation (4 weeks after injury), 4.3% of transplanted E14 spinal progenitors survived when transplanted directly into tubes compared to 0.7% when transplanted into the injury alone. Surviving E14 spinal progenitors exhibited a commitment to the neuronal lineage at 4 weeks post-injury as assessed by both early and late phenotypic markers. Mice receiving tubes with E14 spinal progenitor transplantations had on average 21 ± 4 axons/mm^2 regenerated compared to 8 ± 1 axons/mm^2 for the injury only control which corresponded with a significant increase in remyelination compared to the injury only control, while all conditions exhibited improved forelimb control 4 weeks after injury compared to the injury only. Collectively, we have demonstrated the feasibility of using PEG tubes to modify the implantation site and improve survival of transplanted E14 spinal progenitors.

*Address correspondence to: Courtney M. Dumont, University of Miami, Department of Biomedical Engineering, Phone: (305) 243-6142, cdumont@miami.edu.

Supporting Information Available

The following files are available free of charge:

Figure S1: In vitro E14 spinal progenitors have low GFAP expression

Table S1: Primary antibody clones

Declarations of Interest: None

Graphical Abstract

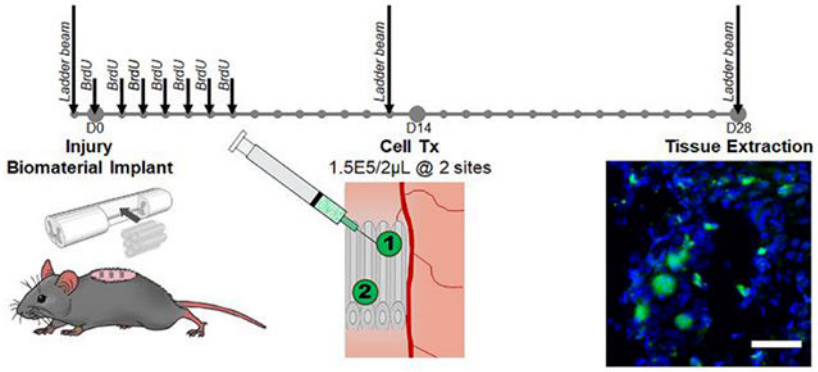

Keywords

spinal cord injury; neural stem cells; biomaterials; tissue engineering

1. Introduction

Traumatic spinal cord injury (SCI) is a particularly debilitating condition that can leave patients paralyzed for the remainder of their lives. Following the primary injury, a secondary injury develops leading to further damage, glial and fibrotic scar formation, and inflammation in the surrounding tissue. Collectively, the barriers from the primary and secondary injury severely limit recovery after SCI. Many current clinical strategies seek to stabilize patients rather than actively promote cell repopulation and tissue regeneration.[1] Exogenous stem cell transplants are one available therapeutic option undergoing Phase I and II clinical trials for numerous applications.[2–7] For SCI, spinal progenitors in rodent models have demonstrated therapeutic potential through integration with endogenous neural circuitry[8–11] and remediation of the extracellular space.[12–23] These studies have provided the foundation for preclinical and clinical trials utilizing human central nervous system progenitors (HuCNS-SCs) for the treatment of SCI.[24] Ultimately, clinical trials evaluating the efficacy of HuCNS-SCs for treatment of SCI in the United States have been unsuccessful, due to poor survival related to stem cell sourcing issues including inconsistencies in scale-up procedures and a lack of *in vivo* validation testing requirements.[24–26]

Stem cell therapies for SCI exhibit poor survival and durability in the spinal cord, limiting the extent and duration of their therapeutic potential. Survival can be cell source dependent, as clinical grade stem cells exhibit decreased transplant survival and recovery compared to research grade stem cells transplanted after SCI.[24] Similarly, we have found stem cell donor age can significantly impact survival, tissue repair, and functional recovery.[27] Apart from cell sourcing, the delivery approach significantly impacts stem cell survival. At 1 week post-transplantation, spinal progenitors typically exhibit a maximum survival rate less than 5% and often times significantly lower.[28–32] Increasing the number of transplanted cells does not lead to a dose dependent increase in transplant survival response.[33, 34] Control over

the injection location by delivering the cells rostral and caudal to the injury can increase transplant survival,[35, 36] but the transplanted cells must migrate into the injury to have their desired effect and neural progenitor cells do not extensively migrate in the central nervous system.[42]. The current gold standard technique is to delay cell transplantation until the inflammatory cytokines decrease within the injury, but with no modification of the inhibitory microenvironment, survival remains low.[37] Inflammatory cytokines like tumor necrosis factor alpha (TNFα), interleukin (IL)-1β, IL-6, and leukemia inhibitory factor (LIF) are important mediators that are strongly activated within the first 12 hours after injury, but decrease by one week after injury.[38–40] Delaying cell transplantation until after this response avoids transplanting into this inflammatory environment opening the potential for increased survival that could improve regenerative potential and functional recovery.[3] These delivery strategies demonstrate that the post-injury microenvironment remains the most important factor in influencing transplant survival. In order to improve survival and actively promote regeneration leading to better functional recovery, control over the pathophysiology of the injury response is required. Developing a system to control the injury microenvironment to shift towards a more hospitable milieu could result in significant regenerative gains.

Exogenous transplants when delivered with biomaterial interventions have demonstrated increases in survival rates. Injectable hydrogels are commonly used as a vehicle for cell transplantation.[43, 44] Cells can be suspended in the liquid state of the gel prior to injection, and then injected and gelled in situ. This is commonly performed at least 7 days after injury[30, 45–47] while in the subacute region (7-14 days after injury) as survival and regeneration have quantitatively been higher compared to acute (<7 days) and chronic models (>14 days).[28, 48, 49] Rigid polymer scaffolds are another example of a combination strategy between biomaterials and cell delivery.[27, 50, 51] Prior to implanting, these scaffolds require cells to be cultured on them *ex vivo*, and then the cell-seeded scaffold is implanted into the injury. These interventions can modify the post-injury microenvironment but lack the ability to have cells transplanted directly into the scaffolds post-implantation. Neither strategy can modify the transplantation site prior to cell delivery, resulting in little opportunity to shift towards a more pro-regenerative environment as transplanted cells arrive.

Previously, we developed a system comprised of a set of hydrogel tubes fabricated through a 2-phase polymerization.[52] An intermediate stage of microspheres controls the macroporosity of the structure before being annealed into a final tube structure. Macroporosity is essential for infiltration of support cells necessary for integration and tissue repair.[53, 54] The hydrogel tubes are approximately 600 μm in diameter and can be cut to the length of the defect, thus allowing multiple tubes to fill a wide range of injury geometries. The inner lumen of the tube is approximately 250 μm and guides axon regrowth, a biophysical and architectural cue that is absent from injected, bulk hydrogels. In an injured spinal cord, the tubes were able to modulate the injury microenvironment by reducing scar formation, limiting inflammatory cells, and promoting endogenous repair.[52]

In this work, we provide the first use of a guidance scaffold to be utilized as an injection site platform for delayed cell delivery. Our previously developed hydrogel tube system will serve as a soft substrate, suitable for delayed injection of enhanced green fluorescent

protein ($EGFP^+$) E14 spinal progenitors into the SCI lesion epicenter two weeks after a C5 lateral hemisection in mice. E14 spinal progenitors were chosen for this application for their improved survival and regeneration compared to adult spinal progenitors.[27] We anticipate the pro-regenerative effects of this biomaterial system will lead to enhanced cell transplantation survival, while also providing flexibility in cell administration timing that is not offered with other SCI guidance systems. In this study, we evaluate the feasibility and early benefits of delayed, direct injection of E14 spinal progenitors into our hydrogel tube system by assessing cell survival, axon elongation and myelination, neurogenesis, and functional recovery serving as an initial step towards a comprehensive cell transplantation platform.

2. Methods

2.1 Fabrication of hydrogel tubes

Hydrogel tubes were generated as previously described.[52] Briefly, 20% w/v 8-arm polyethylene glycol maleimide (PEG-MAL, 20 kDa; JenKem, Plano, TX) was crosslinked with 5 mM slow-degrading-plasmin-sensitive YKND cross-linking peptide (Ac-GCYKNDGCYKNDCG; Genscript, Piscataway, NJ)[55] to form microspheres through water-oil emulsion with diameters ranging between 15 and 150 μm and an average of 45 μm. The PEG-YKND solution was homogenized in silicone oil (Fisher, Hampton, NH) with 2% TWEEN-20 (Sigma, St. Louis, MO) at a speed of 4000 rpm for 1 minute. Microspheres were rinsed by centrifugation three times. Irgacure 2959 photoinitiator (Sigma) dissolved in N-vinylpyrrolidinone (660 mg/mL; Sigma) was added to the microspheres at a final concentration of 1% w/v. The resulting microspheres were then packed into polydimethylsiloxane (PDMS, Dow Corning, Midland, MI) molds to generate PEG tubes (approximate OD: 600 μm, ID: 250 μm, porosity: 66%)and exposed to an ultraviolet lamp for 3 minutes to initiate free radical polymerization. Tubes were rinsed three times, dehydrated, and stored at −80 until use. Tubes were cut to length during surgery to ensure fit within the defect.

2.2 Spinal progenitor isolation

All animal work pertaining to progenitor cell isolation was performed with prior approval and in accordance with the Institutional Animal Care and Use Committee (IACUC) guidelines at the University of Michigan and University of Miami. Embryonic spinal progenitors were isolated from the spinal cords of E14 C57BL/6-Tg(CAG-EGFP)10sb/J mice (Jackson Laboratory, Bar Harbor, ME), enzymatically dissociated with 10 U/mL papain (Worthington, Lakewood, NY) and 37 μg/mL DNase (Sigma) into single cells, and expanded as neurospheres in ultralow attachment flasks (Corning, Corning, NY), as described previously.[27] Embryonic spinal progenitors were expanded in Dulbecco's Modified Eagle Medium (DMEM; Gibco, Grand Island, NY) supplemented with 1X B27 (Gibco), 1X N2 (Gibco), N-acetyl cysteine (NAC; Sigma), and 20 ng/mL basic fibroblast growth factor (FGF2; Peprotech, Rocky Hill, NJ) and leukemia inhibitory factor (LIF; Peprotech). E14 spinal progenitor colonies were passaged with papain as needed and not used beyond the second passage for transplantation studies.

2.3 In vitro assessment of spinal progenitors

E14 spinal progenitors were seeded on PEG hydrogel discs (D = 5 mm, H = 0.5 mm) to assess their survival compatibility with the gels *in vitro*. Due to the macroporosity and 3D nature of our material, PEG discs were used rather than tubes for in vitro experiments as these structures result in better imaging capabilities than tubes *in vitro*. PEG microspheres were fabricated as previously described with the addition of 150 μM of the cell adhesion peptide RGD (GCGYGRGDSPG; Genscript, Piscataway, NJ). Irgacure 2959 photoinitiator was added to the microspheres, and they were pressed into discs between 5 mm round coverslips. The discs were crosslinked by exposure to an ultraviolet lamp for 3 minutes followed by transferring into a 96 well plate. They were then rinsed three times to ensure removal of any excess photoinitiator, sterilized with ethanol, and stored in saline until seeding. E14 spinal progenitor neurospheres were collected, enzymatically dissociated into single cell suspension with papain, and resuspended in supplemented culture media described above. Cells were seeded at 6.5 x 10^4 cells/cm^2 on PEG discs or uncoated tissue culture plastic (TCP). Ethidium homodimer-1 (EthD-1) staining (Life Technologies, Carlsbad, CA, USA) was performed after 24 hours of culture to identify necrotic cell populations. Cells were treated with EthD-1 at a 1:2000 dilution for 15 minutes, after which samples were rinsed three times with sterile phosphate buffered saline (PBS, Life Technologies). Similarly, cell phenotype was assessed with a separate set of cultures (n = 7 samples per condition per time point) after 1 and 3 days of culture. Cells were chemically fixed, permeabilized, and immunostained with mouse anti-Nestin (1:100, Millipore, Burlington, MA) and rabbit anti-GFAP (1:500, Thermo Scientific, Waltham, MA). Samples were imaged with a Nikon Eclipse Ti inverted fluorescent microscope (Nikon, Tokyo, Japan) using a 20X dry objective. Multiple images were averaged per sample, with n = 9 separate TCP wells and n = 9 separate PEG discs over 2 separate trials for viability assessment, while n = 7 PEG or TCP samples were used per time point for phenotype assessment.

2.4 Spinal cord injury surgeries

All animal work was performed with prior approval and in accordance with the Institutional Animal Care and Use Committee (IACUC) guidelines at the University of Michigan. A C5 lateral hemisection spinal cord injury was created in adult C57BL/6J female mice aged 6-8 weeks, as previously described.[56–58] Briefly, mice were anesthetized with 2% isoflurane and provided preemptive local pain management (1 mg kg^{-1} bupivacaine). After confirmation of anesthesia via toe pinch, a 2 cm incision was made in the skin to facilitate the laminectomy performed at C5. A 1.15 mm lateral hemisection was excised in the left side of the spinal cord. This ensures any functional deficits are confined to the left forepaw, providing an internal control with the right paw. PEG tubes were cut to size, allowed to dehydrate for 30 s, and implanted one by one in to the injury site, which accommodated 5 tubes in total. Dehydrating the tubes allows for improved handling and implantation as they are more rigid and easier to handle compared to the fully hydrated tubes. The dehydrated tubes rehydrate once implanted into the injury. Gelfoam was used to secure the injury site in all conditions, after which the muscles were sutured and skin stapled. A subset of mice (no-treatment control group) did not receive an implant but did receive gelfoam over the injured spinal cord. Mice were immediately provided post-operative antibiotics (enrofloxacin 2.5 mg kg^{-1}

once a day for 2 weeks), analgesics (0.1 mg kg^{-1} buprenorphine twice a day for 3 days), and supportive hydration (1 mL 20 g^{-1} lactated ringer solution once a day for 5 days). Bladders were expressed twice daily until function recovered and staples were removed after 10 days. Surgical controls were put in place to limit lesion size variance, including the order of the incisions made to limit the effects of swelling to cut lines, measuring the distance between the rostral and caudal cuts, and verifying the absence of bruising to the contralateral tissue. Exclusion criteria include any deviations to the surgical controls, as well as any variance to the recovery timeline, including an inability to ambulate by post-operative day 3. No mice met these exclusion criteria for this study.

All mice received a second surgery 14 days after the primary injury. Protocols for anesthesia and post-operative care were the same as described with the initial surgery. After anesthesia induction, an incision in the skin was made, sutures in the muscle were removed, and any remaining gelfoam was carefully removed from atop the spinal cord. Two injections of $EGFP^+$ E14 spinal progenitors (2 μL of 150,000 cells in PBS – 300,000 cells/mouse) were injected in the rostral-medial and caudal-lateral regions of the hydrogel implant using a 33G 10μL Hamilton syringe at a rate of 1 μL/minute. Cell transplants were separated into two injections to limit high bolus cell densities that impact necrosis and inhibit cell proliferation after transplantation.[59] The locations were selected to ensure cell distribution along the rostral-caudal and medial-lateral axes to avoid crowding and encourage migration. Gelfoam was placed back over the injury, muscles were sutured, and wound clips applied. Mice were euthanized and spinal cord segments (C4-6) were collected after 4 weeks (2 weeks after cell transplantation). For each condition, n = 4-12 mice at each time point: n = 4 for histology at week 4 (N=16) and n = 12 for ladder beam analysis (N=48).

2.5 Endogenous progenitor identification

Bromodeoxyuridine (BrdU) was used to identify proliferating cells in the first 7 days post-SCI. Intraperitoneal injections of 50 mg/kg BrdU (Roche, Basel, Switzerland) were pulsed every day for 7 days, allowing 7 additional days for unbound BrdU to wash out before exogenous E14 spinal progenitors were implanted, as done by others.[60] In rodent injury models, endogenous neural progenitor populations peak within the first 7 days after injury and gradually decrease with time.[61] As such, a conservative estimate of 7 days post-SCI for daily BrdU injections was chosen for labeling proliferating cells. Any cells that co-localized with BrdU and neuronal lineage markers described below were considered to arise from endogenous spinal progenitors giving rise to new cells along the neuronal lineage. Tissue sections requiring BrdU identification were first denatured in 2N HCl for 1 hour at 37 °C followed by neutralization in 2 five minute rinses of 0.1M borate buffer to facilitate antigen retrieval. Samples were incubated for 1 hour at room temperature in rat anti-BrdU (1:200, Abcam, Cambridge, UK) antibody followed by appropriate fluorophore-conjugated goat anti-rat secondary antibody before proceeding with additional immunohistochemistry of specific cell phenotypes described below.

2.6 Immunohistochemistry

Isolated spinal cords were flash frozen, and then cryosectioned transversely in 12 μm sections. Nine transverse sections chosen for immunohistochemistry analysis were evenly

spaced across the rostral, middle, and caudal (3 sections per region) areas of the tubes and averaged across each animal. In this way, comparisons between animals can be made while also taking into consideration regional differences throughout the injury and tubes, as previously reported.[27] Samples were fixed, permeabilized (0.5% triton-X for 10 minutes) and/or prepared with BrdU staining (described above) as necessary, and incubated overnight at 4°C with primary antibodies. The following antibodies were used for primary detection: rat anti-F4/80 (1:200, Abcam, Cambridge, United Kingdom), goat anti-arginase (1:100, Santa Cruz, Dallas, TX, USA), rabbit anti-neurofilament-200 (1:200, Sigma), goat anti-myelin basic protein (MBP; 1:500, Santa Cruz), chicken anti-P0 (1:250, Aves Labs, Tigard, OR), chicken anti-GFP (1:200, Aves Labs), rabbit anti-GFAP (1:500, Thermo Scientific), rabbit anti-Tuj1 (1:500, Sigma), and mouse anti-NeuN (1:500, Millipore), mouse anti-Nestin (1:200, Millipore). Antibody clones are summarized in Table S1. Species-specific fluorescent secondary antibodies were used for detection at 1:1000 (Life Technologies). Hoechst 33342 (Life Technologies) was used as a counterstain in all tissue sections. Immunostained tissue sections were imaged using an AxioObserver inverted fluorescent microscope (Zeiss, Oberkochen, Germany) using a 10X dry objective.

Progenitor survival, proliferation, and fate: Immunohistochemistry was used to verify no overlap between $BrdU^+$ and $EGFP^+$ cell types. Subpopulations of exogenous $EGFP^+$ cells and endogenous $BrdU^+$ cells were counted manually by two blinded researchers to evaluate progenitor-driven neurogenesis. The following cell populations were quantified: exogenous progenitors ($EGFP^+BrdU^-Nestin^+$), endogenous progenitors ($BrdU^+EGFP^-Nestin^+$), exogenous neuroblasts ($EGFP^+BrdU^-Nestin^+Tuj1^+$), endogenous neuroblasts ($BrdU^+EGFP^-Nestin^+Tuj1^+$), exogenous early neurons ($EGFP^+BrdU^-Tuj1^+Nestin^-$), endogenous early neurons ($BrdU^+EGFP^-Tuj1^+Nestin^-$), exogenous neurons ($EGFP^+BrdU^-NeuN^+$), and endogenous neurons ($BrdU^+EGFP^-NeuN^+$). Cells were quantified within the injury and normalized to the implant or injury (empty control) area. Nine tissues evenly distributed throughout the rostrocaudal axis of the injury were averaged for each animal.

Axon Density and Myelination: Semi-automated counting software, previously described by McCreedy et al.[62], was used to quantify axons and the co-localization of myelin with axons in transverse sections Briefly, the software was calibrated using manual $NF\text{-}200^+$ (axons), $NF\text{-}200^+MBP^+$ (myelinated axons), and $NF\text{-}200^+MBP^+P0^+$ (Schwann cell myelinated axons) counts from a subset of transverse 10X images taken from different animals and regions of the implant. The software then used a series of Hessian filters and threshold functions within the bridge region to reduce noise for selected NF-200, MBP, and P0 images.[62] The software then output total axon counts, as well as the myelinated axon counts based on the curvilinear MBP co-localizing with axons with or without P0 co-localization; image acquisition and analysis was performed by investigators blinded to treatment condition. ImageJ (NIH, Bethesda, MD, USA) was used to analyze all other fluorescent images and define the bridge area. Nine tissues evenly distributed throughout the rostrocaudal axis of the injury were averaged for each animal.

2.7 Locomotor assessment

Horizontal ladder beam was used to evaluate mouse locomotor function and coordination over a 4 week period post-SCI, as previously described for all conditions (N=48, 12 per condition).[63] Each of the 50 rungs were numbered and equally spaced along the length of the beam with a dark enclosure containing bedding at the far end of the apparatus. An HD Handycam camcorder (Sony, Tokyo, Japan) was used to record mouse ambulation across ladderbeam. Mice were acclimated to the ladder beam over three sessions in the two weeks preceding the initial surgery. Baseline scores were determined to separate animals in to equal groups (tubes or gelfoam) prior to the initial surgery. Mice were evaluated on the ladder beam every 2 weeks over the course of the experiment. The 2 week evaluation occurred prior to the second surgery in which the mice received E14 spinal progenitors or vehicle (PBS) injections. This was to allow researchers to separate animals in equal groups prior to the addition of cell transplants. Observation and ladder beam scoring were performed by two blinded observers for 3 trials per animal. Animals were scored by average forepaw full placement on the ladder beam during the task.

2.8 Statistics

Data normality was assessed using a Shapiro-Wilk normality test with an α value of 0.05, which determined parametric statistical tests were appropriate for our analyses. Multiple comparison pairs were analyzed using a one-way or two-way ANOVA with Tukey post-hoc test. All statistics test significance using an α value of 0.05. For all graphs, * denotes $p < 0.05$ compared to SCI only and ^ denotes $p < 0.05$ compared to E14 spinal progenitors only unless otherwise noted in the figure caption. ROUT tests were performed with a false discovery rate of 1% to identify any outliers in data. All values are reported as mean ± standard error of the mean (SEM). Prism 7 (GraphPad Software, La Jolla, CA) software was used for all data analysis.

3. Results

3.1 E14 spinal progenitors are viable and maintain Nestin$^+$ phenotype on PEG in vitro

E14 spinal progenitors were cultured on PEG hydrogels *in vitro* as an initial assessment to model their viability once they are later injected into tubes *in vivo*. PEG hydrogels have a demonstrated history of biocompatibility, and here we show that the E14 spinal progenitors can attach to the surface of our PEG hydrogels. Cells were seeded on PEG hydrogel discs functionalized with RGD adhesion peptide and uncoated tissue culture plastic (TCP) as a control. Necrosis was assessed by staining for dead cells using EthD-1 one day after seeding. Both the TCP (Figure 1A) and the PEG hydrogel (Figure 1B) exhibited high viability ($EGFP^+EthD\text{-}1^-$) of the seeded progenitors. Viability was 98.5 ± 0.5% for the TCP and 97.4 ± 0.9% for the PEG hydrogel with no significant difference (p=0.2379) between the two (Figure 1C). Additionally, migratory cell phenotypes were observed on the hydrogels indicating the seeded cells are spreading along the surface. Nestin expression, indicating uncommitted stem and progenitor phenotypes, was assessed one (Figure 1D, E) and three days (Figure 1G, H) after seeding for both conditions. Total $EGFP^+$ cell density was determined on Day 1 (51.4 ± 3.4 and 33.8 ± 5.0 cells/mm^2) and Day 3 (36.6 ± 6.3 and 38.6 ± 7.6 cells/mm^2) for TCP and PEG conditions, respectively (Figure 1F). Co-expression

of Nestin with EGFP was assessed as a percent of total $EGFP^+$ cells. On Day 1 $Nestin^+$ cells were 74.6 ± 2.7% and 78.3 ± 4.6% of the $EGFP^+$ cells for TCP and PEG, respectively. On Day 3 $Nestin^+$ cells were 81.3 ± 2.7% and 76.2 ± 2.1% of the $EGFP^+$ cells for TCP and PEG, respectively (Figure 1I). No significant differences were observed across day or condition for EGFP density (p=0.1963) or Nestin commitment (p=0.5338). Seeded cells that were $GFAP^+Nestin^+$ and $GFAP^+Nestin^-$ were also quantified (Figure S1). There were no significant differences across either condition or day for both cell types.

3.2 E14 spinal progenitor survival improves when injected into hydrogel tubes

Immediately following injury, five hydrogel tubes were implanted into the C5 lateral hemisection injury. Each individual hydrogel tube was fabricated to have an inner diameter of 250 μm and an outer diameter of 600 μm as shown imaged longitudinally (Figure 2A) and transversely (Figure 2B) where the white lines denote the inner lumen. Two weeks after injury and tube implantation, mice received two injections of 150,000 $EGFP^+$ E14 spinal progenitors. After another two weeks (4 weeks post-injury) spinal cords were collected and evaluated histologically for survival of transplanted E14 spinal progenitors. Conditions included in this study were tubes with (Tubes + E14) and without (Tubes) E14 spinal progenitor delivery, E14 spinal progenitor delivery only (E14), and an injury only control (SCI). $EGFP^+$ cells were observed in both conditions receiving progenitor transplants (Figure 2C–D). Mice receiving cells transplanted directly into the injury site had on average 20.3 ± 7.5 cells/mm^2 while those receiving cells transplanted into hydrogel tubes had on average 44.1 ± 3.8 cells/mm^2, (Figure 2E). Similarly, an increase in average percent survival of the 300,000 transplanted cells was observed in mice receiving tubes with E14 spinal progenitors (4.3%) as compared to the E14 spinal progenitor only condition (0.7%) (Figure 2F).

3.3 Transplanted E14 spinal progenitor proliferation increases when delivered into tubes

Proliferating neuronal lineage cells in the injury region were classified into two categories: endogenous and exogenous. Endogenous stem cells were identified through IP injections of BrdU administered for 1 week following injury. After the 1 week of BrdU administration, a 1 week buffer time served to ensure any unbound BrdU was excreted prior to exogenous transplant delivery.[64] At two weeks, exogenous E14 spinal progenitors were transplanted into two sites in the integrated tubes (Figure 3A). Staining for $Nestin^+$ progenitors was performed on tissue isolated at 4 weeks (Figure 3B), and co-localization of $Nestin^+$ cells with either BrdU (Figure 3C) or EGFP (Figure 3E) and DAPI (Figure 3F) was used to determine the endogenous or exogenous source of neural progenitors, respectively. Overlays of Nestin staining showed no overlap between $EGFP^+$ and $BrdU^+$ progenitors (Figure 3H, I, J). Exogenous $EGFP^+Nestin^+$ E14 spinal progenitors had a significantly (p=0.028) higher density (5.3 ± 1.4 cells/mm^2) when transplanted into tubes compared to direct transplantation (1.1 ± 0.3 cells/mm^2) into the injury site (Figure 3D). Endogenous progenitors were present throughout all conditions, including those absent of exogenous cell transplants. No significant differences (p=0.144) were observed between SCI only (11.9 ± 2.5 cells/mm^2), E14 only (18.1 ± 2.6 cells/mm^2), Tubes (13.7 ± 1.4 cells/mm^2), and Tubes + E14 (9.2 ± 2.8 cells/mm^2) conditions (Figure 3G).

3.4 Transplanted E14 spinal progenitors commit to a neuronal lineage

Progenitor fate along the neuronal lineage was characterized for both exogenous and endogenous populations in the injury region. Progenitor source was identified by $EGFP^+$ (exogenous) or $BrdU^+$ (endogenous) colocalization with neuronal markers as described previously, and early commitment to the neuronal lineage was assessed with Nestin and Tuj1. $Nestin^+Tuj1^+$ neuroblasts and $Tuj1^+Nestin^-$ early neurons were observed in both exogenous (Figure 4A) and endogenous (Figure 4D) cell populations. In the exogenous group, no significant difference was present between E14 spinal progenitor delivery with and without tubes for neuroblast density (Figure 4B); however, a significantly higher density of early neurons was present in the injury site when transplanted into tubes (Figure 4C). The combined neuronal lineage committed (early neurons and neuroblasts) accounted for 8.0 ± 5.1% of transplanted cells, while 7.6 ± 0.9% remained uncommitted ($Nestin^+Tuj^-$) when progenitors were delivered with the tubes. The endogenous group exhibited no significant differences across any of the conditions in neuroblast (Figure 4E) or early neuron (Figure 4F) densities. More mature $NeuN^+$ neurons were also observed to arise from both progenitor sources (Figure 4G), albeit in lower densities than early neurons and neuroblasts. The exogenous progenitors had a significantly greater density (1.5 ± 0.5 cells/mm^2) when transplanted directly into tubes compared to transplantation directly into the injury (0 ± 0 cells/mm^2) (Figure 4H). No difference in newly formed endogenous $NeuN^+$ cells was observed across conditions (Figure 4I).

3.5 Hydrogel tubes facilitate improved early axon elongation and remyelination

At 4 weeks post-injury, all conditions were evaluated histologically for axon elongation through the injury site, in addition to their corresponding myelination (Figure 5A–D). $NF\text{-}200^+$ axons were observed in transverse sections along the length of the injury for all conditions. Mice receiving tubes either with (158 ± 14 axons/mm^2) or without (182 ± 11 axons/mm^2) E14 spinal progenitors exhibited a robust increase in axon density compared to the E14 spinal progenitors only (115 ± 5 axons/mm^2) and SCI only (69 ± 8 axons/mm^2) control conditions. Additionally, E14 spinal progenitors exhibited a moderate increase in axon density compared to injury control only (Figure 5E).

Regenerated axons were further characterized by assessing the extent and source of their myelination. A significant increase in $NF\text{-}200^+MBP^+$ myelinated axon density was observed in animals receiving tubes alone and tubes with E14 spinal progenitors compared to E14 spinal progenitors only and SCI controls (Figure 5F). Tubes with E14 spinal progenitors had 21 ± 4 myelinated axons/mm^2 while tubes alone had 25 ± 4 myelinated axons/mm^2, whereas the E14 spinal progenitors only and SCI only had 8 ± 0.6 myelinated axons/mm^2 and 8 ± 1 myelinated axons/mm^2, respectively. Myelination source of $NF\text{-}200^+MBP^+$ axons was characterized by staining for $P0^+$ Schwann cell derived myelin and calculated as a percent of total myelinated axons. A significantly higher percent of axons was myelinated by Schwann cells in tubes with E14 spinal progenitors (77 ± 3%) and tubes alone (68 ± 7%) compared to E14 spinal progenitors (49 ± 5%) and SCI only (45 ± 0.3%) (Figure 5G).

3.6 Functional recovery improves over time following implantation and transplantation

Functional recovery of the animals was tested using a horizontal ladder beam test to assess ipsilateral forelimb function and coordination. All animals were trained to walk across the beam prior to injury, and their return to function was assessed over 4 weeks. The average number of successful steps increased for all conditions over the testing period (Figure 6). At 4 weeks post-injury, all experimental conditions had significantly more placements on average compared to the injury only control demonstrating the biomaterial implant and transplanted progenitors independently support regeneration, however, additive functional recovery beyond that achieved with each condition alone was not observed over this recovery period.

4. Discussion

In this work, we expanded the functionality of our axonal growth guidance PEG hydrogel tubes to additionally serve as an implanted substrate for delayed stem cell transplantation. The tubes alone promote endogenous repair mechanisms, leading to an inflammatory shift and thus a more pro-regenerative microenvironment post-SCI.[52] They also can modulate the host response to create a pro-regenerative environment for stem cell injection. Neural stem cells have the potential to improve regeneration leading to improved functional recovery through endogenous cell replacement, neurotrophin and proteoglycan release, and immunomodulatory cytokine recruitment, but that potential is limited greatly by their survival post-transplantation.[65] While the immune system attempts to clear the injury site of damaged neurons and glia, cell transplants are exposed to cytotoxic cytokines leading to their poor survival and diminished returns on function. Implantation of the hydrogel tubes into the injured spinal cord can mitigate this response and improve progenitor transplant survival. To demonstrate the feasibility of this system, we implanted tubes immediately following a cervical hemisection injury into the created lesion. Upon implantation, they integrated with surrounding tissue and shifted the host response while promoting repair for two weeks. After the two weeks of microenvironment remediation by the tubes, E14 spinal progenitors were injected directly into the integrated tubes that then also served as a privileged injection site for cell transplantation. Through this combination therapy, we were able to develop a tunable system for cell transplantation that has the potential to further enhance recovery post-SCI.

Biomaterials provide structural support and physical attachment sites for progenitor cell transplantation, leading to improved survival and tissue regeneration.[30, 46, 66–69] Rigid scaffolds and hydrogels both provide support for transplanted cells, mitigating cell death attributed to anoikis during bolus cell injections. Additionally, biomaterials can limit necrosis associated with injection techniques as cells are loaded onto rigid scaffolds prior to implantation,[27, 70, 71] or, in the case of hydrogels, the cell membranes are protected from shear forces by the biomaterial.[72, 73] These protective strategies can be engineered into a number of biomaterial vehicles, however, the ability of the material to guide the regeneration process should also be considered. Highly porous, multichannel poly(lactide-*co*-glycolide) (PLG) bridges, previously be used to deliver spinal progenitor cells,[27] are formed into a rigid structure with longitudinal channels that provide directional guidance cues for axonal

regrowth through the scaffold. Similarly, electrospun poly ε-caprolactone scaffolds can be used to directionally orient tissue growth post-SCI and cultured with stem cells.[71] In both cases, improved regeneration was observed, but the mechanical properties of the scaffolds and their inability to mold to unique injury anatomy limit translatability. Conversely, hydrogel vehicles for cell delivery better match native tissue mechanical properties, and once in the injury site, can conform to injury anatomy. Stem cells can be suspended in hydrogels prior to injection, and the combination can be delivered simultaneously.[43, 44] Mothe et al. used a hyaluronan and methyl cellulose based hydrogel blend suspended with neural stem cells and injected them into a rat contusion injury. Their hydrogel blend improved survival compared to the neural stem cells delivered in culture media alone, and the blend reduced cavitation observed in control conditions.[30] An added benefit of delivering stem cells suspended in a hydrogel is their protection offered against shear forces typically exerted on the stem cells when injecting. Cai et al. developed a shear-thinning hydrogel (SHIELD) that significantly improved adipose stem cell transplant survival[72] and was later applied to Schwann cell transplantation for SCI therapy.[73] While the mechanical, injury-shaping, and shear stress protecting properties of hydrogel-based delivery mechanisms are advantageous, they lack the directional cues seen with rigid polymer implants that are important for the directional regrowth in the spinal cord. Our system presently does not co-deliver our cell transplants within a hydrogel, as suggested above, as we chose to focus on providing a platform to remediate the transplantation environment prior to cell transplantation instead protective strategies during transplantation. To do this, we combine the mechanical and injury-matching properties of soft hydrogels with the directionality seen in rigid polymers. To do this, we use PEG hydrogel tubes with a compressive modulus (12.5 kPa) in the range of the spared spinal cord (1-300 kPa) surrounding the lesion.[52] Unlike rigid polymer scaffolds, our hydrogel tube system is a composite of multiple individual units making it modular, rather than a single implant structure that is the basis of traditional preformed scaffolds. Our modular tube system is soft enough to be cut and combined to fit various patient injury anatomies, while the lumens of the tubes direct tissue regrowth, providing a defined path that is absent with traditional hydrogel scaffolds. Furthermore, drying the tubes prior to implantation leads to tube swelling upon implantation, resulting in an improved fit to injury anatomy as opposed to a rigid implant that will not change shape once *in vivo*. Importantly, the tubes also provide a soft substrate for the direct, minimally invasive injection of exogenous stem cells into the injury allowing for control over the location of transplantation which is crucial for engraftment.[49]

Many biomaterial strategies have been designed to protect stem cell transplants during delivery to improve post-transplant survival and stem cell-mediated regeneration. PLG bridges cultured with E14 spinal progenitors had a survival of ~5% at 1 week post-transplantation, but this dropped precipitously over time to 0.3% at 8 weeks and eventually 0% at the final 6 month timepoint.[27] The hyaluronan-based blend was delivered 9 days after initial injury and exhibited approximately a 1.2% survival 1 week post-transplantation that dropped to 0.05% at 8 weeks.[30] Schwann cell-containing SHIELD hydrogels were injected 14 days after injury and their survival was assessed at 2 days and 4 weeks post-transplantation. An overall survival percent was not presented in this study at these timepoints, but a marked increase compared to stem cells delivered in saline only was

observed.[73] These strategies, however, offer little control over when the stem cells are delivered to the injury site relative to the biomaterial, as they either have to be cultured on the scaffolds or encapsulated in the hydrogel solution prior to implantation. By making stem cell delivery dependent on biomaterial delivery, there is no opportunity to address other barriers to stem cell survival or regeneration. One such barrier is the inflammation associated with immune cell infiltration and glial scar formation leading to poor transplant survival and engraftment. Many biomaterials, including the PLG bridges previously used to delivery spinal progenitors, have demonstrated immune and glial modulation properties in numerous rodent models,[27, 54, 74–76] however, their ability to confer this protection to cell transplants is limited when delivered simultaneously. Delaying the transplant survival, as opposed to implanting a cell-biomaterial composite immediately after injury, opens the opportunity to modulate the immune response prior to cell injection leading to an improved chance of survival and regeneration. Delaying stem cell transplantation to overcome inflammation is not a novel concept, as stem cell therapies without biomaterials have relied on this technique to improve initial stem cell survival.[37] However, what is novel, is to combine delayed administration strategies with a biomaterial known to remediate the inflammatory injury milieu to create a more hospitable transplant site. For this study, we delayed our transplant delivery to 2 weeks post-tube implantation, and survival was assessed 2 weeks post-transplantation (4 weeks post-tube implantation) at the injury site. Transplant survival was 4.3% when injected into tubes, similar to the PLG bridges and significantly greater than the hyaluronan hydrogels despite assessment a week later,[27, 30] when cell survival would have continued to decrease. It is possible that survival is under-reported due to cell survival, however, neural progenitor cells do not migrate extensively *in vivo*,[42] especially not by our 2 week quantification timepoint. Furthermore, we did not observe any migration of our transplanted progenitors into the contralateral tissue when we quantified surviving cell densities. The delayed injection allowed the tubes to begin to shift the injury paradigm prior to implantation and thus facilitated survival and improved transplant longevity demonstrating a combinatorial benefit of this platform beyond that observed with strategies developing biomaterials as a delivery vehicle.

In addition to survival, the tubes aided in increasing the neuronal lineage commitment of the transplanted cells. One possible explanation of the neuronal increase is that the tubes provided improved microenvironment control, resulting in a decreased presence of inflammatory cytokines. Numerous pro-inflammatory cytokines have been linked with SCI and other central nervous system diseases.[79] The increased expression of TNFα, IL-6, and IL-1β is known to limit neurogenesis.[80] In particular, IL-6 has been shown to cause neural stem cells to preferentially differentiate along astroglial lineages, limiting their neurogenic potential.[81–83] The increased presence of cells committed to the neuronal lineage and the demonstrated ability of the tubes to resolve transient increases of IL-6-producing inflammatory cells in previous studies,[52] suggests that the tubes can be used as a transplant site for progenitor cells that is supportive of neurogenesis through inflammatory cytokine remediation. Because this was a proof-of-concept study for determining the feasibility of transplanting cells into our tubes, we did not characterize the observed cytokine profile pre- and post-implantation of the tubes. Moving forward, RT-PCR experiments could be performed to identify cytokine presence as a function of tube implantation.

With that information, we could better optimize cell delivery time to match with downregulation of pro-inflammatory cytokines. Furthermore, future studies could further leverage biomaterial-mediated regulation of the microenvironment through the controlled release of anti-inflammatory cytokines and neurotrophic factors from the tubes. Previous lentiviral-mediated overexpression of anti-inflammatory and neurotrophic factors from PLG bridges have shown regenerative improvements,[84–86] and their delivery can be applied to these tubes.

While transplanted progenitors were mostly neuronal committed, approximately 7.6% remained uncommitted at the early 2 week assessment point. From a differentiation timeline standpoint, this is expected as neural progenitor neuronal commitment takes approximately two weeks of differentiation *in vivo*, so it would be expected that exactly at 2 weeks there would remain some uncommitted cells.[87] Zahir et al. implanted subepyndymal region-isolated neural stem/progenitor-coated tubes into a T8 transection and evaluated differentiation after 5 weeks, at which point they observed 18.3% of their cells remained $Nestin^+$ and uncommitted to the neuron, astrocyte, and oligodendrocyte markers they selected.[88] Additionally, neural progenitor cells can serve roles beyond solely repopulating lost or damaged cells post-SCI. They have the potential to mediate regulatory functions important for limiting secondary injury in the spinal cord. These include limiting glial scarring and increasing remyelination of newly formed axons.[47] Moreover, they can actively promote regeneration through release of numerous neurotrophic factors, growth factors, and extracellular proteins.[16, 17] It should be noted, that we anticipate a large portion of exogenous and endogenous cells give rise to astrocytes, which can immunostain positive for Nestin and may account for a subset of these seemingly uncommitted cells. However, further evaluation of these cells with GFAP would not bring additional closure to this possibility, as progenitor cells of the central nervous system and astrocytes are both known to co-express Nestin and GFAP. [77, 78]

Infiltration of endogenous stem cells and their neuronal lineage commitment were also evaluated by labeling proliferating cells with BrdU for 7 days post-SCI and identifying localization with neuronal lineage markers. It is likely that endogenous stem cells entering the injury will differentiate along an astroglial lineage, as there is a degree of overlap in cell markers at this stage. With that in mind, we decided to focus on cell phenotypes associated with neurogenesis rather than astrocytes. This also allowed us to assume that $BrdU^+$ cells co-staining with our markers were from endogenous progenitor pools. Activation of these endogenous stem cells could potentially further enhance recovery post-SCI, but there has been significant debate as to whether endogenous neurogenesis is possible after SCI. Through the use of a neurotrophin-loaded chitosan tube Yang et al. have shown that newly formed endogenous neurons can be observed.[60] Similarly, Liu et al. fabricated a self-assembling peptide nanofiber hydrogel loaded with growth factor cocktail that demonstrated endogenous neurogenesis corresponding to significant increases in functional recovery beginning six weeks after implantation.[89] While we observed newly formed neurons from an endogenous source after SCI using similar techniques, no significant differences were observed across conditions for any of the quantified cell populations along the neuronal linage at 4 weeks post-injury. It is possible that our endogenous progenitor identification provided an underestimate, but we chose to stop labeling after 7 days as endogenous

neural progenitors typically peak in rodent models within the first 7 days post-SCI.[60, 61] Furthermore, this provided ample time for excess BrdU to wash out, preventing any overlap in labeling with our exogenous transplants. Both of the cited studies that did observe increased endogenous neurogenesis used therapeutic-loaded biomaterials in their injury repair models. Our study did not incorporate any therapeutics into our tubes, but in future experiments neurotrophic delivery from the tubes will be utilized for their potential for enhancing endogenous neurogenesis.

For this work, a cervical lateral hemisection was employed rather than the thoracic hemisection model reported previously,[52] which was done to increase translatability as cervical SCI has a higher incidence than thoracic SCI.[90, 91] In the previous thoracic model, the macroporous tubes provided guidance cues through the injured region for new axons and supported remyelination of these newly formed axons.[52] The findings from this study are consistent with previous axon elongation and remyelination results demonstrating repeatability across different SCI models. Mice receiving tubes, either with or without E14 spinal progenitors, had a significant increase in axon density and myelinated axon density compared to the E14 spinal progenitor only and SCI only controls at 4 weeks post-implantation. Ladder beam scores between mice receiving tubes with E14 spinal progenitors and tubes only did not vary significantly from each other, and by 4 weeks they both had a significant increase in stepping compared to the injury only control. The combination of the histological and functional data presented here strongly suggests that the transplantation did not have an adverse effect on the regenerative abilities of the tubes, nor were the benefits of the progenitors and tubes additive at the time points evaluated. Much of the regeneration process, including sparing, plasticity, and axon growth, may have initiated immediately after tube implantation. Thus, most of the effects observed would be a direct result of tube implantation, as the stem cells were not implanted until halfway through the recovery period. This delay, while crucial for survival, may have dampened the discernible effect of the transplanted cells as regeneration was tube-dominated. Shortening the delay window by mitigating the inflammatory response quicker and delivering stem cells earlier could allow them to have a significant impact early on. It is also possible that synergistic effects between the tubes and stem cells could be observed at later timepoints that would quantified through histological and functional assessments. Notably, the increased survival and durability of the progenitors reported in this study will be instrumental in enabling synergistic improvements at later time points.

5. Conclusion

Biomaterial and exogenous stem cell combination strategies have previously shown initial success in improving cell transplant survival. With previously used strategies, a lack of control over the delivery timeline of stem cells independent from the biomaterial implantation limited the flexibility of transplant strategies. These biomaterial conduits must modulate the surrounding environment at the same time as delivering stem cells, resulting in transplanted cells entering an inhospitable microenvironment. The major advance of this work provides an alternative strategy, where initially implanting a soft hydrogel created a more permissive injection site for a delayed cell transplantation. The hydrogel served as a soft substrate for a minimally invasive injection of E14 spinal progenitors into the injury.

To our knowledge, this work is the first to demonstrate a step-wise combinatorial approach using progenitor cells and biomaterials for SCI to enhance progenitor cell survival.

Supplementary Material

Refer to Web version on PubMed Central for supplementary material.

Acknowledgments

This work was supported by the NIH (R01EB005678)

References

1. Fehlings MG; Tetreault LA; Wilson JR; Kwon BK; Burns AS; Martin AR; Hawryluk G; Harrop JS, A Clinical Practice Guideline for the Management of Acute Spinal Cord Injury: Introduction, Rationale, and Scope. Global Spine J 2017, 7 (3 Suppl), 84S–94S, doi: 10.1177/2192568217703387.
2. Howard D; Buttery LD; Shakesheff KM; Roberts SJ, Tissue engineering: strategies, stem cells and scaffolds. J Anat 2008, 213 (1), 66–72, doi: 10.1111/j.1469-7580.2008.00878.x. [PubMed: 18422523]
3. Kwon SG; Kwon YW; Lee TW; Park GT; Kim JH, Recent advances in stem cell therapeutics and tissue engineering strategies. Biomater Res 2018, 22, 36–36, doi: 10.1186/s40824-018-0148-4. [PubMed: 30598836]
4. Wang Y; Yin P; Bian G-L; Huang H-Y; Shen H; Yang J-J; Yang Z-Y; Shen Z-Y, The combination of stem cells and tissue engineering: an advanced strategy for blood vessels regeneration and vascular disease treatment. Stem Cell Res Ther 2017, 8 (1), 194–194, doi: 10.1186/s13287-017-0642-y. [PubMed: 28915929]
5. Kalladka D; Sinden J; Pollock K; Haig C; McLean J; Smith W; McConnachie A; Santosh C; Bath PM; Dunn L; Muir KW, Human neural stem cells in patients with chronic ischaemic stroke (PISCES): a phase 1, first-in-man study. Lancet 2016, 388 (10046), 787–796, doi: 10.1016/S0140-6736(16)30513-X. [PubMed: 27497862]
6. Squillaro T; Peluso G; Galderisi U, Clinical Trials with Mesenchymal Stem Cells: An Update. Cell Transplant 2016, 25 (5), 829–848, doi: 10.3727/096368915X689622. [PubMed: 26423725]
7. Song WK; Park K-M; Kim H-J; Lee JH; Choi J; Chong SY; Shim SH; Del Priore LV; Lanza R, Treatment of macular degeneration using embryonic stem cell-derived retinal pigment epithelium: preliminary results in Asian patients. Stem Cell Rep 2015, 4 (5), 860–872, doi: 10.1016/j.stemcr.2015.04.005.
8. Lien BV; Tuszynski MH; Lu P, Astrocytes migrate from human neural stem cell grafts and functionally integrate into the injured rat spinal cord. Exp Neurol 2019, 314, 46–57, doi: 10.1016/j.expneurol.2019.01.006. [PubMed: 30653967]
9. Kumamaru H; Kadoya K; Adler AF; Takashima Y; Graham L; Coppola G; Tuszynski MH, Generation and post-injury integration of human spinal cord neural stem cells. Nat Methods 2018, 15 (9), 723–731, doi: 10.1038/s41592-018-0074-3. [PubMed: 30082899]
10. Lu P; Gomes-Leal W; Anil S; Dobkins G; Huie JR; Ferguson AR; Graham L; Tuszynski M, Origins of Neural Progenitor Cell-Derived Axons Projecting Caudally after Spinal Cord Injury. Stem Cell Rep 2019, 13 (1), 105–114, doi: 10.1016/j.stemcr.2019.05.011.
11. Lu P; Ceto S; Wang Y; Graham L; Wu D; Kumamaru H; Staufenberg E; Tuszynski MH, Prolonged human neural stem cell maturation supports recovery in injured rodent CNS. Journal of Clin Invest 2017, 127 (9), 3287–3299, doi: 10.1172/JCI92955.
12. Dumont CM; Margul DJ; Shea LD, Tissue Engineering Approaches to Modulate the Inflammatory Milieu following Spinal Cord Injury. Cells Tissues Organs 2016, 202 (1–2), 52–66, doi: 10.1159/000446646. [PubMed: 27701152]

13. Hawryluk GWJ; Mothe A; Wang J; Wang S; Tator C; Fehlings MG, An in vivo characterization of trophic factor production following neural precursor cell or bone marrow stromal cell transplantation for spinal cord injury. Stem Cells and Dev 2012, 21 (12), 2222–2238, doi: 10.1089/scd.2011.0596.

14. Lu P; Jones LL; Snyder EY; Tuszynski MH, Neural stem cells constitutively secrete neurotrophic factors and promote extensive host axonal growth after spinal cord injury. Exp Neurol 2003, 181 (2), 115–129, doi: 10.1016/S0014-4886(03)00037-2. [PubMed: 12781986]

15. Lladó J; Haenggeli C; Maragakis NJ; Snyder EY; Rothstein JD, Neural stem cells protect against glutamate-induced excitotoxicity and promote survival of injured motor neurons through the secretion of neurotrophic factors. Mol Cell Neurosci 2004, 27 (3), 322–331, doi: 10.1016/j.mcn.2004.07.010. [PubMed: 15519246]

16. Li Q; Ford MC; Lavik EB; Madri JA, Modeling the neurovascular niche: VEGF- and BDNF-mediated cross-talk between neural stem cells and endothelial cells: An in vitro study. J Neurosci Res 2006, 84 (8), 1656–1668, doi: 10.1002/jnr.21087. [PubMed: 17061253]

17. Kamei N; Tanaka N; Oishi Y; Hamasaki T; Nakanishi K; Sakai N; Ochi M, BDNF NT-3, and NGF Released From Transplanted Neural Progenitor Cells Promote Corticospinal Axon Growth in Organotypic Cocultures. Spine (Philadelphia) 2007, 32 (12), 1272–1278, doi: 10.1097/BRS.0b013e318059afab.

18. Laterza C; Merlini A; De Feo D; Ruffini F; Menon R; Onorati M; Fredrickx E; Muzio L; Lombardo A; Comi G; Quattrini A; Taveggia C; Farina C; Cattaneo E; Martino G, iPSC-derived neural precursors exert a neuroprotective role in immune-mediated demyelination via the secretion of LIF. Nat Commun 2013, 4 (1), 2597, doi: 10.1038/ncomms3597. [PubMed: 24169527]

19. Campos LS; Leone DP; Relvas JB; Brakebusch C; Fässler R; Suter U; ffrench-Constant C, β1 integrins activate a MAPK signalling pathway in neural stem cells that contributes to their maintenance. Development 2004, 131 (14), 3433–3444, doi: 10.1242/dev.01199. [PubMed: 15226259]

20. Gurok U; Steinhoff C; Lipkowitz B; Ropers HH; Scharff C; Nuber UA, Gene expression changes in the course of neural progenitor cell differentiation. J Neurosci 2004, 24 (26), 5982–6002, doi: 10.1523/JNEUROSCI.0809-04.2004. [PubMed: 15229246]

21. Gu W-L; Fu S-L; Wang Y-X; Li Y; Lü H-Z; Xu X-M; Lu P-H, Chondroitin sulfate proteoglycans regulate the growth, differentiation and migration of multipotent neural precursor cells through the integrin signaling pathway. BMC Neurosci 2009, 10, 128–128, doi: 10.1186/1471-2202-10-128. [PubMed: 19845964]

22. Sirko S; von Holst A; Wizenmann A; Götz M; Faissner A, Chondroitin sulfate glycosaminoglycans control proliferation, radial glia cell differentiation and neurogenesis in neural stem/progenitor cells. Development 2007, 134 (15), 2727, doi: 10.1242/dev.02871. [PubMed: 17596283]

23. von Holst A; Sirko S; Faissner A, The unique 473HD-Chondroitinsulfate epitope is expressed by radial glia and involved in neural precursor cell proliferation. J Neurosci 2006, 26 (15), 4082–4094, doi: 10.1523/JNEUROSCI.0422-06.2006. [PubMed: 16611825]

24. Anderson AJ; Piltti KM; Hooshmand MJ; Nishi RA; Cummings BJ, Preclinical Efficacy Failure of Human CNS-Derived Stem Cells for Use in the Pathway Study of Cervical Spinal Cord Injury. Stem Cell Rep 2017, 8 (2), 249–263, doi: 10.1016/j.stemcr.2016.12.018.

25. Levi AD; Anderson KD; Okonkwo DO; Park P; Bryce TN; Kurpad SN; Aarabi B; Hsieh J; Gant K, Clinical Outcomes from a Multi-Center Study of Human Neural Stem Cell Transplantation in Chronic Cervical Spinal Cord Injury. Journal Neurotrauma 2018, 36 (6), 891–902, doi: 10.1089/neu.2018.5843.

26. Temple S; Studer L, Lessons Learned from Pioneering Neural Stem Cell Studies. Stem Cell Rep 2017, 8 (2), 191–193, doi: 10.1016/j.stemcr.2017.01.024.

27. Dumont CM; Munsell MK; Carlson MA; Cummings BJ; Anderson AJ; Shea LD, Spinal Progenitor-Laden Bridges Support Earlier Axon Regeneration Following Spinal Cord Injury. Tissue Eng, Part A 2018, 24 (21–22), 1588–1602, doi: 10.1089/ten.TEA.2018.0053. [PubMed: 30215293]

28. Tetzlaff W; Okon EB; Karimi-Abdolrezaee S; Hill CE; Sparling JS; Plemel JR; Plunet WT; Tsai EC; Baptiste D; Smithson LJ; Kawaja MD; Fehlings MG; Kwon BK, A systematic review of

cellular transplantation therapies for spinal cord injury. Journal Neurotrauma 2011, 28 (8), 1611–1682, doi: 10.1089/neu.2009.1177.

29. Parr AM; Kulbatski I; Zahir T; Wang X; Yue C; Keating A; Tator CH, Transplanted adult spinal cord–derived neural stem/progenitor cells promote early functional recovery after rat spinal cord injury. J Neurosci 2008, 155 (3), 760–770, doi: 10.1016/j.neuroscience.2008.05.042.
30. Mothe AJ; Tam RY; Zahir T; Tator CH; Shoichet MS, Repair of the injured spinal cord by transplantation of neural stem cells in a hyaluronan-based hydrogel. Biomaterials 2013, 34 (15), 3775–3783, doi: 10.1016/j.biomaterials.2013.02.002. [PubMed: 23465486]
31. Cusimano M; Biziato D; Brambilla E; Donegà M; Alfaro-Cervello C; Snider S; Salani G; Pucci F; Comi G; Garcia-Verdugo JM; De Palma M; Martino G; Pluchino S, Transplanted neural stem/precursor cells instruct phagocytes and reduce secondary tissue damage in the injured spinal cord. Brain : a journal of neurology 2012, 135 (Pt 2), 447–460, doi: 10.1093/brain/awr339. [PubMed: 22271661]
32. Butenschön J; Zimmermann T; Schmarowski N; Nitsch R; Fackelmeier B; Friedemann K; Radyushkin K; Baumgart J; Lutz B; Leschik J, PSA-NCAM positive neural progenitors stably expressing BDNF promote functional recovery in a mouse model of spinal cord injury. Stem Cell Research & Therapy 2016, 7, 11–11, doi: 10.1186/s13287-015-0268-x. [PubMed: 26762640]
33. Bonnamain V; Neveu I; Naveilhan P, Neural stem/progenitor cells as a promising candidate for regenerative therapy of the central nervous system. Frontiers in cellular neuroscience 2012, 6, 17–17, doi: 10.3389/fncel.2012.00017. [PubMed: 22514520]
34. Cooke MJ; Vulic K; Shoichet MS, Design of biomaterials to enhance stem cell survival when transplanted into the damaged central nervous system. Soft Matter 2010, 6 (20), 4988–4998, doi: 10.1039/C0SM00448K.
35. Nagoshi N; Khazaei M; Ahlfors J-E; Ahuja CS; Nori S; Wang J; Shibata S; Fehlings MG, Human Spinal Oligodendrogenic Neural Progenitor Cells Promote Functional Recovery After Spinal Cord Injury by Axonal Remyelination and Tissue Sparing. Stem cells translational medicine 2018, 7 (11), 806–818, doi: 10.1002/sctm.17-0269. [PubMed: 30085415]
36. Chen J; Bernreuther C; Dihné M; Schachner M, Cell Adhesion Molecule L1–Transfected Embryonic Stem Cells with Enhanced Survival Support Regrowth of Corticospinal Tract Axons in Mice after Spinal Cord Injury. Journal of neurotrauma 2005, 22 (8), 896–906, doi: 10.1089/neu.2005.22.896. [PubMed: 16083356]
37. Karimi-Abdolrezaee S; Eftekharpour E; Wang J; Morshead CM; Fehlings MG, Delayed Transplantation of Adult Neural Precursor Cells Promotes Remyelination and Functional Neurological Recovery after Spinal Cord Injury. The Journal of Neuroscience 2006, 26 (13), 3377, doi: 10.1523/JNEUROSCI.4184-05.2006. [PubMed: 16571744]
38. Shamash S; Reichert F; Rotshenker S, The cytokine network of Wallerian degeneration: tumor necrosis factor-alpha, interleukin-1alpha, and interleukin-1beta. The Journal of neuroscience : the official journal of the Society for Neuroscience 2002, 22 (8), 3052–3060, doi: 10.1523/JNEUROSCI.22-08-03052.2002. [PubMed: 11943808]
39. Lacroix S; Chang L; Rose-John S; Tuszynski MH, Delivery of hyper-interleukin-6 to the injured spinal cord increases neutrophil and macrophage infiltration and inhibits axonal growth. J Comp Neurol 2002, 454 (3), 213–28, doi: 10.1002/cne.10407. [PubMed: 12442313]
40. Donnelly DJ; Popovich PG, Inflammation and its role in neuroprotection, axonal regeneration and functional recovery after spinal cord injury. Experimental Neurology 2008, 209 (2), 378–388, doi: 10.1016/j.expneurol.2007.06.009. [PubMed: 17662717]
41. Liu B; Gao HM; Wang JY; Jeohn GH; Cooper CL; Hong JS, Role of nitric oxide in inflammation-mediated neurodegeneration. Ann N Y Acad Sci 2002, 962, 318–31, doi: 10.1111/j.1749-6632.2002.tb04077.x. [PubMed: 12076984]
42. Rosenzweig ES; Brock JH; Lu P; Kumamaru H; Salegio EA; Kadoya K; Weber JL; Liang JJ; Moseanko R; Hawbecker S; Huie JR; Havton LA; Nout-Lomas YS; Ferguson AR; Beattie MS; Bresnahan JC; Tuszynski MH, Restorative effects of human neural stem cell grafts on the primate spinal cord. Nature medicine 2018, 24 (4), 484–490, doi: 10.1038/nm.4502.
43. Marquardt LM; Heilshorn SC, Design of Injectable Materials to Improve Stem Cell Transplantation. Current stem cell reports 2016, 2 (3), 207–220, doi: 10.1007/s40778-016-0058-0. [PubMed: 28868235]

44. Liang K; Bae KH; Kurisawa M, Recent advances in the design of injectable hydrogels for stem cell-based therapy. Journal of Materials Chemistry B 2019, 7 (24), 3775–3791, doi: 10.1039/C9TB00485H.

45. Geissler SA; Sabin AL; Besser RR; Gooden OM; Shirk BD; Nguyen QM; Khaing ZZ; Schmidt CE, Biomimetic hydrogels direct spinal progenitor cell differentiation and promote functional recovery after spinal cord injury. Journal of neural engineering 2018, 15 (2), 025004–025004, doi: 10.1088/1741-2552/aaa55c. [PubMed: 29303112]

46. Führmann T; Tam RY; Ballarin B; Coles B; Elliott Donaghue I; van der Kooy D; Nagy A; Tator CH; Morshead CM; Shoichet MS, Injectable hydrogel promotes early survival of induced pluripotent stem cell-derived oligodendrocytes and attenuates longterm teratoma formation in a spinal cord injury model. Biomaterials 2016, 83, 23–36, doi: 10.1016/j.biomaterials.2015.12.032. [PubMed: 26773663]

47. Cummings BJ; Uchida N; Tamaki SJ; Salazar DL; Hooshmand M; Summers R; Gage FH; Anderson AJ, Human neural stem cells differentiate and promote locomotor recovery in spinal cord-injured mice. Proceedings of the National Academy of Sciences of the United States of America 2005, 102 (39), 14069, doi: 10.1073/pnas.0507063102. [PubMed: 16172374]

48. Cheng I; Park DY; Mayle RE; Githens M; Smith RL; Park HY; Hu SS; Alamin TF; Wood KB; Kharazi AI, Does timing of transplantation of neural stem cells following spinal cord injury affect outcomes in an animal model? Journal of spine surgery (Hong Kong) 2017, 3 (4), 567–571, doi: 10.21037/jss.2017.10.06. [PubMed: 29354733]

49. Piltti KM; Salazar DL; Uchida N; Cummings BJ; Anderson AJ, Safety of epicenter versus intact parenchyma as a transplantation site for human neural stem cells for spinal cord injury therapy. Stem cells translational medicine 2013, 2 (3), 204–216, doi: 10.5966/sctm.2012-0110. [PubMed: 23413374]

50. Shin JE; Jung K; Kim M; Hwang K; Lee H; Kim I-S; Lee BH; Lee I-S; Park KI, Brain and spinal cord injury repair by implantation of human neural progenitor cells seeded onto polymer scaffolds. Experimental & Molecular Medicine 2018, 50 (4), 39, doi: 10.1038/s12276-018-0054-9.

51. Koffler J; Zhu W; Qu X; Platoshyn O; Dulin JN; Brock J; Graham L; Lu P; Sakamoto J; Marsala M; Chen S; Tuszynski MH, Biomimetic 3D-printed scaffolds for spinal cord injury repair. Nature medicine 2019, 25 (2), 263–269, doi: 10.1038/s41591-018-0296-z.

52. Dumont CM; Carlson MA; Munsell MK; Ciciriello AJ; Strnadova K; Park J; Cummings BJ; Anderson AJ; Shea LD, Aligned hydrogel tubes guide regeneration following spinal cord injury. Acta Biomater 2019, 86, 312–322, doi: 10.1016/j.actbio.2018.12.052. [PubMed: 30610918]

53. Thomas AM; Kubilius MB; Holland SJ; Seidlits SK; Boehler RM; Anderson AJ; Cummings BJ; Shea LD, Channel density and porosity of degradable bridging scaffolds on axon growth after spinal injury. Biomaterials 2013, 34 (9), 2213–2220, doi: 10.1016/j.biomaterials.2012.12.002. [PubMed: 23290832]

54. Yang Y; Laporte LD; Zelivyanskaya ML; Whittlesey KJ; Anderson AJ; Cummings BJ; Shea LD, Multiple Channel Bridges for Spinal Cord Injury: Cellular Characterization of Host Response. Tissue Engineering Part A 2009, 15 (11), 3283–3295, doi: 10.1089/ten.tea.2009.0081. [PubMed: 19382871]

55. Shikanov A; Smith RM; Xu M; Woodruff TK; Shea LD, Hydrogel network design using multifunctional macromers to coordinate tissue maturation in ovarian follicle culture. Biomaterials 2011, 32 (10), 2524–31, doi: 10.1016/j.biomaterials.2010.12.027. [PubMed: 21247629]

56. Margul DJ; Park J; Boehler RM; Smith DR; Johnson MA; McCreedy DA; He T; Ataliwala A; Kukushliev TV; Liang J; Sohrabi A; Goodman AG; Walthers CM; Shea LD; Seidlits SK, Reducing neuroinflammation by delivery of IL-10 encoding lentivirus from multiple-channel bridges. Bioeng Transl Med 2016, 1 (2), 136–148, doi: 10.1002/btm2.10018. [PubMed: 27981242]

57. Thomas AM; Kubilius MB; Holland SJ; Seidlits SK; Boehler RM; Anderson AJ; Cummings BJ; Shea LD, Channel density and porosity of degradable bridging scaffolds on axon growth after spinal injury. Biomaterials 2013, 34 (9), 2213–20, doi: 10.1016/j.biomaterials.2012.12.002. [PubMed: 23290832]

58. Thomas AM; Seidlits SK; Goodman AG; Kukushliev TV; Hassani DM; Cummings BJ; Anderson AJ; Shea LD, Sonic hedgehog and neurotrophin-3 increase oligodendrocyte numbers and

myelination after spinal cord injury. Integr Biol (Camb) 2014, 6 (7), 694–705, doi: 10.1039/c4ib00009a. [PubMed: 24873988]

59. Piltti KM; Avakian SN; Funes GM; Hu A; Uchida N; Anderson AJ; Cummings BJ, Transplantation dose alters the dynamics of human neural stem cell engraftment, proliferation and migration after spinal cord injury. Stem Cell Res 2015, 15 (2), 341–53, doi: 10.1016/j.scr.2015.07.001. [PubMed: 26298025]
60. Yang Z; Zhang A; Duan H; Zhang S; Hao P; Ye K; Sun YE; Li X, NT3-chitosan elicits robust endogenous neurogenesis to enable functional recovery after spinal cord injury. Proc Natl Acad Sci U S A 2015, 112 (43), 13354–9, doi: 10.1073/pnas.1510194112. [PubMed: 26460015]
61. Mao Y; Mathews K; Gorrie CA, Temporal Response of Endogenous Neural Progenitor Cells Following Injury to the Adult Rat Spinal Cord. Frontiers in cellular neuroscience 2016, 10, 58–58, doi: 10.3389/fncel.2016.00058. [PubMed: 27013972]
62. McCreedy DA; Margul DJ; Seidlits SK; Antane JT; Thomas RJ; Sissman GM; Boehler RM; Smith DR; Goldsmith SW; Kukushliev TV; Lamano JB; Vedia BH; He T; Shea LD, Semi-automated counting of axon regeneration in poly(lactide co-glycolide) spinal cord bridges. J Neurosci Methods 2016, 263, 15–22, doi: 10.1016/j.jneumeth.2016.01.021. [PubMed: 26820904]
63. Cummings BJ; Engesser-Cesar C; Cadena G; Anderson AJ, Adaptation of a ladder beam walking task to assess locomotor recovery in mice following spinal cord injury. Behav Brain Res 2007, 177 (2), 232–41, doi: 10.1016/j.bbr.2006.11.042. [PubMed: 17197044]
64. Matiašová A; Ševc J; Mikeš J; Jendželovský R; Daxnerová Z; Fedoročko P, Flow cytometric determination of 5-bromo-2′-deoxyuridine pharmacokinetics in blood serum after intraperitoneal administration to rats and mice. Histochemistry and Cell Biology 2014, 142 (6), 703–712, doi: 10.1007/s00418-014-1253-7. [PubMed: 25059651]
65. Pereira IM; Marote A; Salgado AJ; Silva NA, Filling the Gap: Neural Stem Cells as A Promising Therapy for Spinal Cord Injury. Pharmaceuticals (Basel, Switzerland) 2019, 12 (2), 65, doi: 10.3390/ph12020065.
66. Gojgini S; Tokatlian T; Segura T, Utilizing Cell–Matrix Interactions To Modulate Gene Transfer to Stem Cells Inside Hyaluronic Acid Hydrogels. Molecular Pharmaceutics 2011, 8 (5), 1582–1591, doi: 10.1021/mp200171d. [PubMed: 21823632]
67. Seidlits SK; Liang J; Bierman RD; Sohrabi A; Karam J; Holley SM; Cepeda C; Walthers CM, Peptide-modified, hyaluronic acid-based hydrogels as a 3D culture platform for neural stem/progenitor cell engineering. Journal of Biomedical Materials Research Part A 2019, 107 (4), 704–718, doi: 10.1002/jbm.a.36603. [PubMed: 30615255]
68. Li X; Dai J, Bridging the gap with functional collagen scaffolds: tuning endogenous neural stem cells for severe spinal cord injury repair. Biomaterials Science 2018, 6 (2), 265–271, doi: 10.1039/C7BM00974G. [PubMed: 29265131]
69. Katoh H; Yokota K; Fehlings MG, Regeneration of Spinal Cord Connectivity Through Stem Cell Transplantation and Biomaterial Scaffolds. Frontiers in cellular neuroscience 2019, 13, 248–248, doi: 10.3389/fncel.2019.00248. [PubMed: 31244609]
70. Olson HE; Rooney GE; Gross L; Nesbitt JJ; Galvin KE; Knight A; Chen B; Yaszemski MJ; Windebank AJ, Neural stem cell- and Schwann cell-loaded biodegradable polymer scaffolds support axonal regeneration in the transected spinal cord. Tissue engineering. Part A 2009, 15 (7), 1797–1805, doi: 10.1089/ten.tea.2008.0364. [PubMed: 19191513]
71. Terraf P; Kouhsari SM; Ai J; Babaloo H, Tissue-Engineered Regeneration of Hemisected Spinal Cord Using Human Endometrial Stem Cells, Poly ε-Caprolactone Scaffolds, and Crocin as a Neuroprotective Agent. Molecular Neurobiology 2017, 54 (7), 5657–5667, doi: 10.1007/s12035-016-0089-7. [PubMed: 27624387]
72. Cai L; Dewi RE; Heilshorn SC, Injectable Hydrogels with In Situ Double Network Formation Enhance Retention of Transplanted Stem Cells. Advanced functional materials 2015, 25 (9), 1344–1351, doi: 10.1002/adfm.201403631. [PubMed: 26273242]
73. Marquardt LM; Doulames VM; Wang AT; Dubbin K; Suhar RA; Kratochvil MJ; Medress ZA; Plant GW; Heilshorn SC, Designer, injectable gels to prevent transplanted Schwann cell loss during spinal cord injury therapy. Science Advances 2020, 6 (14), eaaz1039, doi: 10.1126/sciadv.aaz1039. [PubMed: 32270042]

74. Tuinstra HM; Aviles MO; Shin S; Holland SJ; Zelivyanskaya ML; Fast AG; Ko SY; Margul DJ; Bartels AK; Boehler RM; Cummings BJ; Anderson AJ; Shea LD, Multifunctional, multichannel bridges that deliver neurotrophin encoding lentivirus for regeneration following spinal cord injury. Biomaterials 2012, 33 (5), 1618–1626, doi: 10.1016/j.biomaterials.2011.11.002. [PubMed: 22130565]

75. Tuinstra HM; Margul DJ; Goodman AG; Boehler RM; Holland SJ; Zelivyanskaya ML; Cummings BJ; Anderson AJ; Shea LD, Long-Term Characterization of Axon Regeneration and Matrix Changes Using Multiple Channel Bridges for Spinal Cord Regeneration. Tissue Engineering Part A 2013, 20 (5–6), 127–1037, doi: 10.1089/ten.tea.2013.0111.

76. Pawar K; Cummings BJ; Thomas A; Shea LD; Levine A; Pfaff S; Anderson AJ, Biomaterial bridges enable regeneration and re-entry of corticospinal tract axons into the caudal spinal cord after SCI: Association with recovery of forelimb function. Biomaterials 2015, 65, 1–12, doi: 10.1016/j.biomaterials.2015.05.032. [PubMed: 26134079]

77. Codega P; Silva-Vargas V; Paul A; Maldonado-Soto AR; Deleo AM; Pastrana E; Doetsch F, Prospective identification and purification of quiescent adult neural stem cells from their in vivo niche. Neuron 2014, 82 (3), 545–59, doi: 10.1016/j.neuron.2014.02.039. [PubMed: 24811379]

78. Pastrana E; Cheng L-C; Doetsch F, Simultaneous prospective purification of adult subventricular zone neural stem cells and their progeny. Proceedings of the National Academy of Sciences 2009, 106 (15), 6387, doi: 10.1073/pnas.0810407106.

79. Stammers AT; Liu J; Kwon BK, Expression of inflammatory cytokines following acute spinal cord injury in a rodent model. Journal of Neuroscience Research 2012, 90 (4), 782–790, doi: 10.1002/jnr.22820. [PubMed: 22420033]

80. Carpentier PA; Palmer TD, Immune influence on adult neural stem cell regulation and function. Neuron 2009, 64 (1), 79–92, doi: 10.1016/j.neuron.2009.08.038. [PubMed: 19840551]

81. Taga T; Fukuda S, Role of IL-6 in the neural stem cell differentiation. Clinical Reviews in Allergy & Immunology 2005, 28 (3), 249–256, doi: 10.1385/CRIAI:28:3:249. [PubMed: 16129909]

82. Nakamura M; Okada S; Toyama Y; Okano H, Role of IL-6 in spinal cord injury in a mouse model. Clinical Reviews in Allergy & Immunology 2005, 28 (3), 197–203, doi: 10.1385/CRIAI:28:3:197. [PubMed: 16129904]

83. Guptarak J; Wanchoo S; Durham-Lee J; Wu Y; Zivadinovic D; Paulucci-Holthauzen A; Nesic O, Inhibition of IL-6 signaling: A novel therapeutic approach to treating spinal cord injury pain. PAIN 2013, 154 (7), doi:

84. Smith DR; Dumont CM; Park J; Ciciriello AJ; Guo A; Tatineni R; Cummings BJ; Anderson AJ; Shea LD, Polycistronic Delivery of IL-10 and NT-3 Promotes Oligodendrocyte Myelination and Functional Recovery in a Mouse Spinal Cord Injury Model. Tissue Engineering Part A 2020, doi: 10.1089/ten.tea.2019.0321.

85. Margul DJ; Park J; Boehler RM; Smith DR; Johnson MA; McCreedy DA; He T; Ataliwala A; Kukushliev TV; Liang J; Sohrabi A; Goodman AG; Walthers CM; Shea LD; Seidlits SK, Reducing neuroinflammation by delivery of IL-10 encoding lentivirus from multiple-channel bridges. Bioengineering & Translational Medicine 2016, 1 (2), 136–148, doi: 10.1002/btm2.10018. [PubMed: 27981242]

86. Park J; Decker JT; Margul DJ; Smith DR; Cummings BJ; Anderson AJ; Shea LD, Local Immunomodulation with Anti-inflammatory Cytokine-Encoding Lentivirus Enhances Functional Recovery after Spinal Cord Injury. Molecular Therapy 2018, 26 (7), 1756–1770, doi: 10.1016/j.ymthe.2018.04.022. [PubMed: 29778523]

87. Tao Y; Zhang S-C, Neural Subtype Specification from Human Pluripotent Stem Cells. Cell stem cell 2016, 19 (5), 573–586, doi: 10.1016/j.stem.2016.10.015. [PubMed: 27814479]

88. Zahir T; Nomura H; Guo XD; Kim H; Tator C; Morshead C; Shoichet M, Bioengineering neural stem/progenitor cell-coated tubes for spinal cord injury repair. Cell Transplant 2008, 17 (3), 245–54, doi: 10.3727/096368908784153887. [PubMed: 18522228]

89. Liu H; Xu X; Tu Y; Chen K; Song L; Zhai J; Chen S; Rong L; Zhou L; Wu W; So K-F; Ramakrishna S; He L, Engineering Microenvironment for Endogenous Neural Regeneration after Spinal Cord Injury by Reassembling Extracellular Matrix. ACS Applied Materials & Interfaces 2020, 12 (15), 17207–17219, doi: 10.1021/acsami.9b19638. [PubMed: 32207300]

90. Singh A; Tetreault L; Kalsi-Ryan S; Nouri A; Fehlings MG, Global prevalence and incidence of traumatic spinal cord injury. Clinical epidemiology 2014, 6, 309–331, doi: 10.2147/CLEP.S68889. [PubMed: 25278785]

91. Pickett GE; Campos-Benitez M; Keller JL; Duggal N, Epidemiology of Traumatic Spinal Cord Injury in Canada. Spine 2006, 31 (7), 799–805, doi: 10.1097/01.brs.0000207258.80129.03. [PubMed: 16582854]

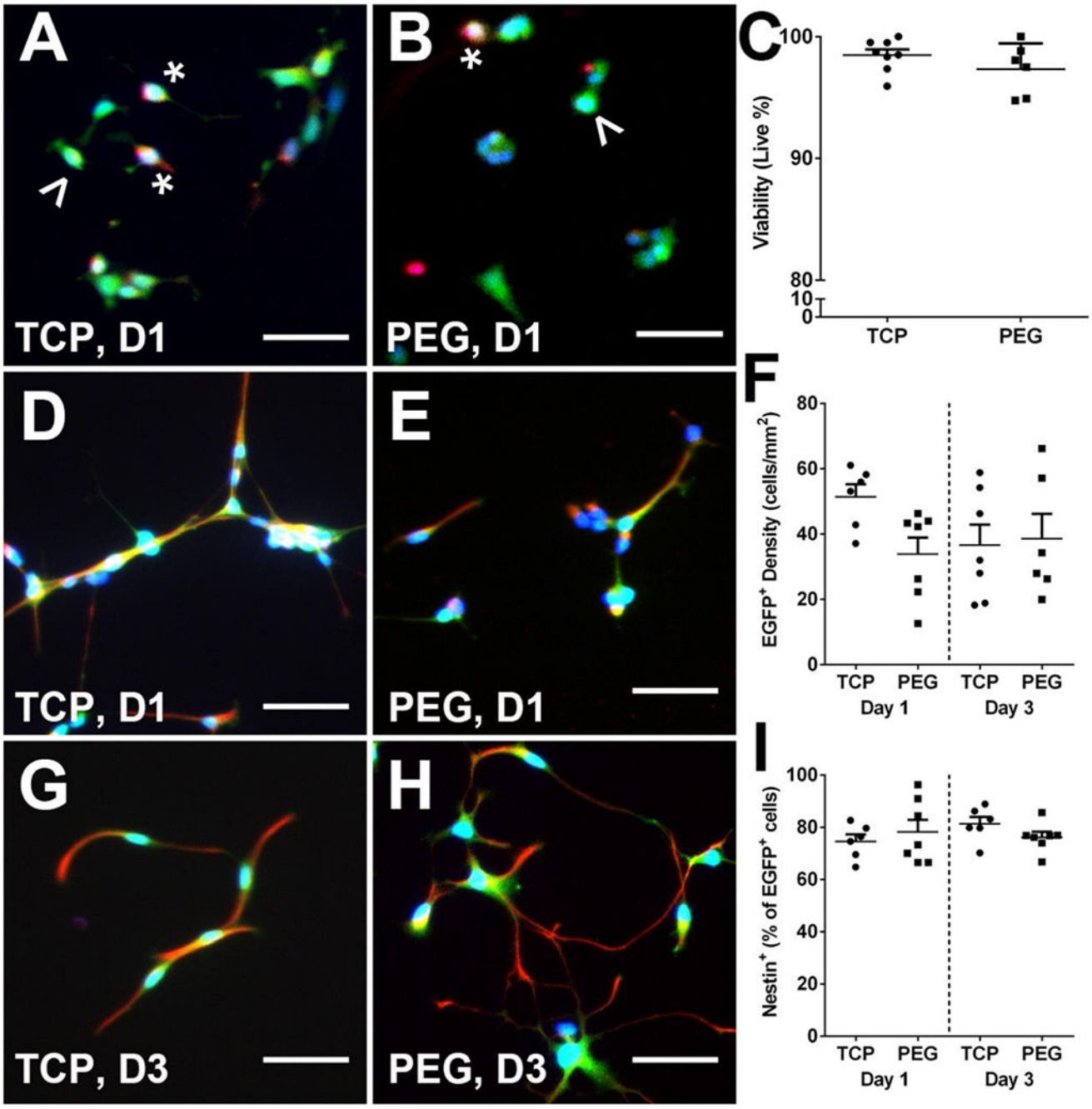

Fig. 1.

E14 spinal progenitors have high viability and Nestin expression when cultured on fabricated PEG hydrogels. Cell viability on Day 1 was determined by seeding EGFP$^+$ E14 spinal progenitors (green) on TCP (A) and PEG (B) and viability was assessed using ethidium homodimer-1 (red, A and B, denoted by *) for dead cells. Migratory cell phenotypes (denoted by ^) were observed in both conditions. Quantitatively, viability was assessed as a percent of live cells out of total cells present (C). Nestin$^+$ (red, D-H) EGFP$^+$ cells were observed in both conditions on Days 1 (D, E) and 3 (G, H) after seeding.

Total $EGFP^+$ density (F) and Nestin expression (I) as a percent of $EGFP^+$ cells were assessed. No significant differences were observed for viability, $EGFP^+$ density, or Nestin expressioncommitment. n=6-8, 50 μm scale bars.

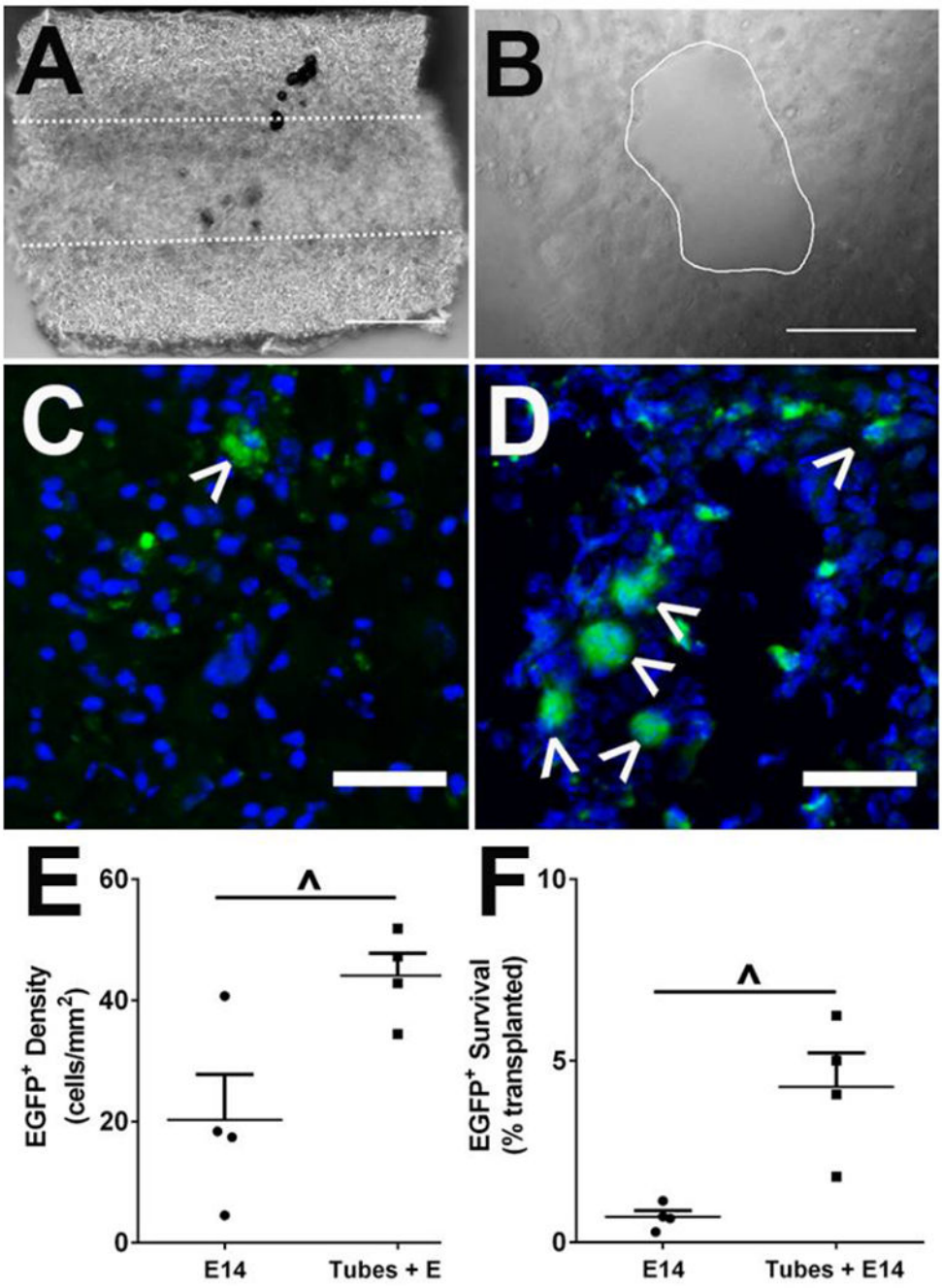

Fig. 2.

Delayed transplantation of EGFP$^+$ spinal progenitors directly into tubes 2 weeks post-injury improves survival. Five hydrogel tubes were implanted directly after lateral C5 hemisection injury. A sample tube shown imaged longitudinally (A) and transversely (B). EGFP$^+$ spinal progenitors were transplanted 2 weeks post-injury into the injury site alone (C) or into tubes at the injury (D) and imaged in transverse sections at 4 weeks post-injury. Quantitatively, survival was assessed 4 weeks post-injury (2 weeks post-transplantation), and an increase in cell density (E) and survival (F) from total transplanted population indicates improved

survival for spinal progenitors with a delayed injection into tubes. Data are presented as mean ± SEM. n=4 per condition, ^ $p<0.05$, 50 μm scale bars.

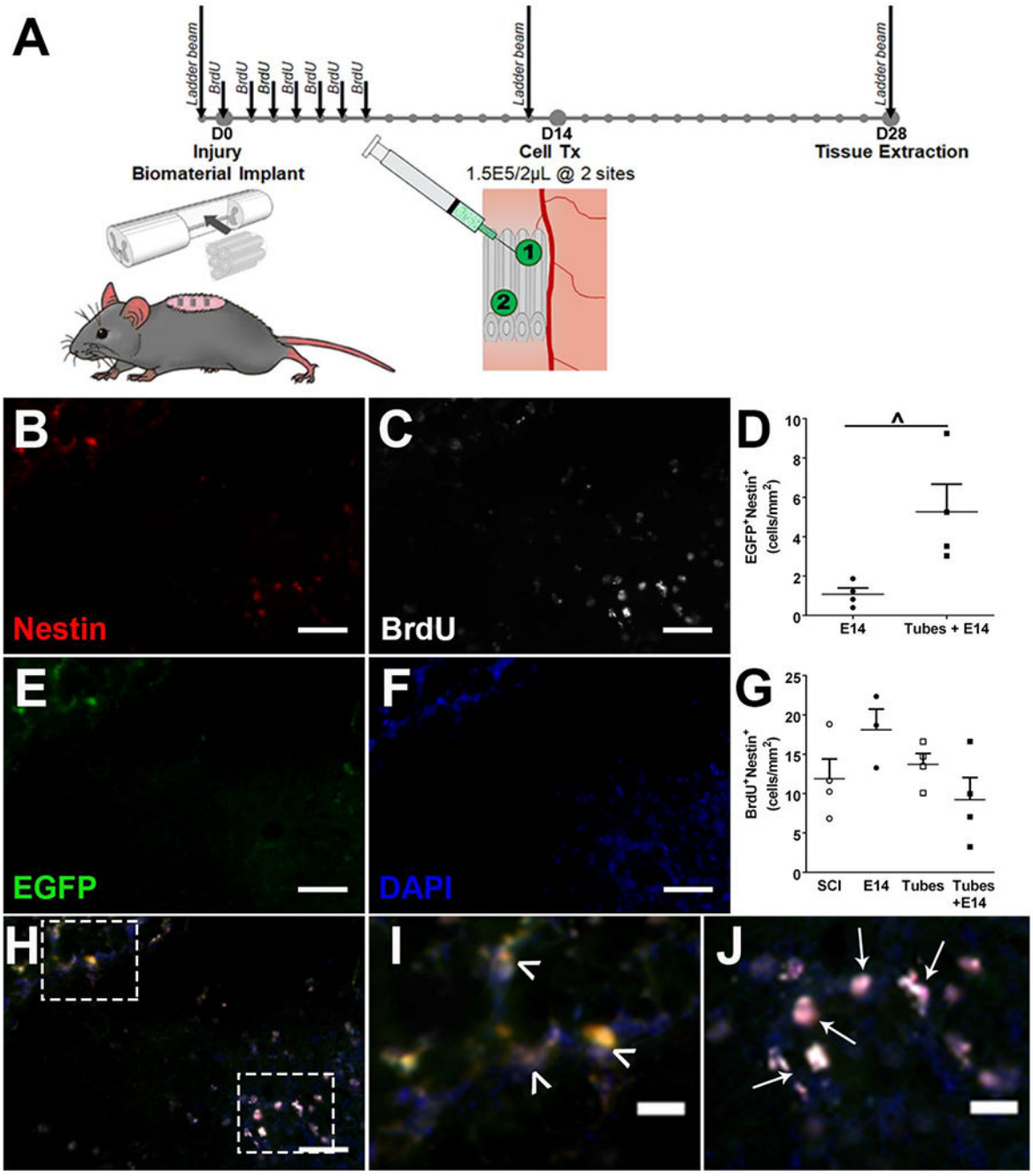

Fig. 3.

Experimental timeline detailed with surgical interventions, BrdU injections, and functional testing timepoints (A). Immunofluorescent staining for Nestin$^+$ (B), BrdU$^+$ (C), EGFP$^+$ (E) cells to identify progenitor populations with DAPI (F) as a nuclear stain. Identified progenitors (Nestin$^+$, red) were classified in two groups as either endogenous (BrdU$^+$Nestin$^+$, denoted by ↑) or exogenous (EGFP$^+$ Nestin$^+$, denoted by ^) with no observed overlap between groups (H, I, J). Quantitatively, tubes with transplanted spinal progenitors had an increase in exogenous progenitor density (D) while there was no

significant difference in endogenous progenitor density across conditions (G). n=4 per condition, ^ $p<0.05$, 200 μm scale bars (B, C, E, F, H) 10 μm scale bars (I, J). Representative sample for Tubes + E14 condition shown.

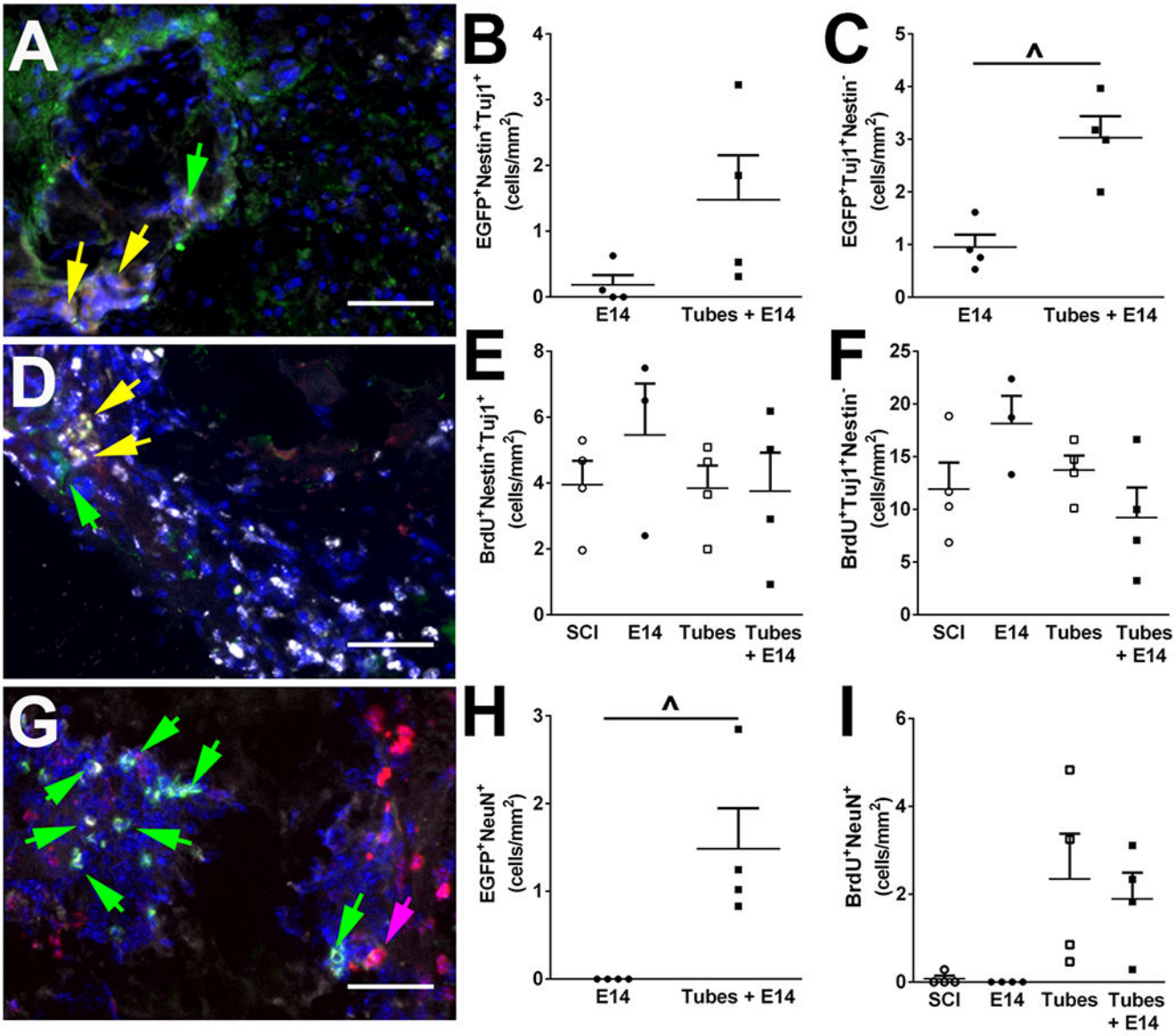

Fig. 4.

Endogenous and exogenous progenitors differentiate along a neuronal cell lineage. Exogenous cells (grey, A) differentiation in to neuroblasts ($Nestin^+Tuj1^+$|red^+green^+, yellow arrow) or immature neurons ($Tuj1^+Nestin^-$|green only, green arrow) was assessed by immunofluorescence. No significant difference was observed for exogenously derived neuroblasts (B), but exogenously derived immature neurons were increased when spinal progenitors were delivered in the tubes compared to cell only condition (C). Similarly, endogenous progenitors identified with BrdU (grey, D) were evaluated for neuroblasts ($Nestin^+Tuj1^+$|red^+green^+, yellow arrow) or immature neurons ($Tuj1^+Nestin^-$|green only, green arrow). No significant difference across conditions were observed for endogenous neuroblasts (E) or endogenous immature neuron formation (F). Mature $NeuN^+$ neurons (grey, G) were also observed to arise from both exogenous (EGFP, green, green arrow) and endogenous (BrdU, red, pink arrow) cells. Exogenous transplants had a significantly greater

density of mature neurons when delivered into tubes (H) while endogenous progenitors exhibited no differences in conditions (I). n=4 per condition, ^ $p<0.05$, 50 μm scale bars. Representative samples for Tubes + E14 condition shown.

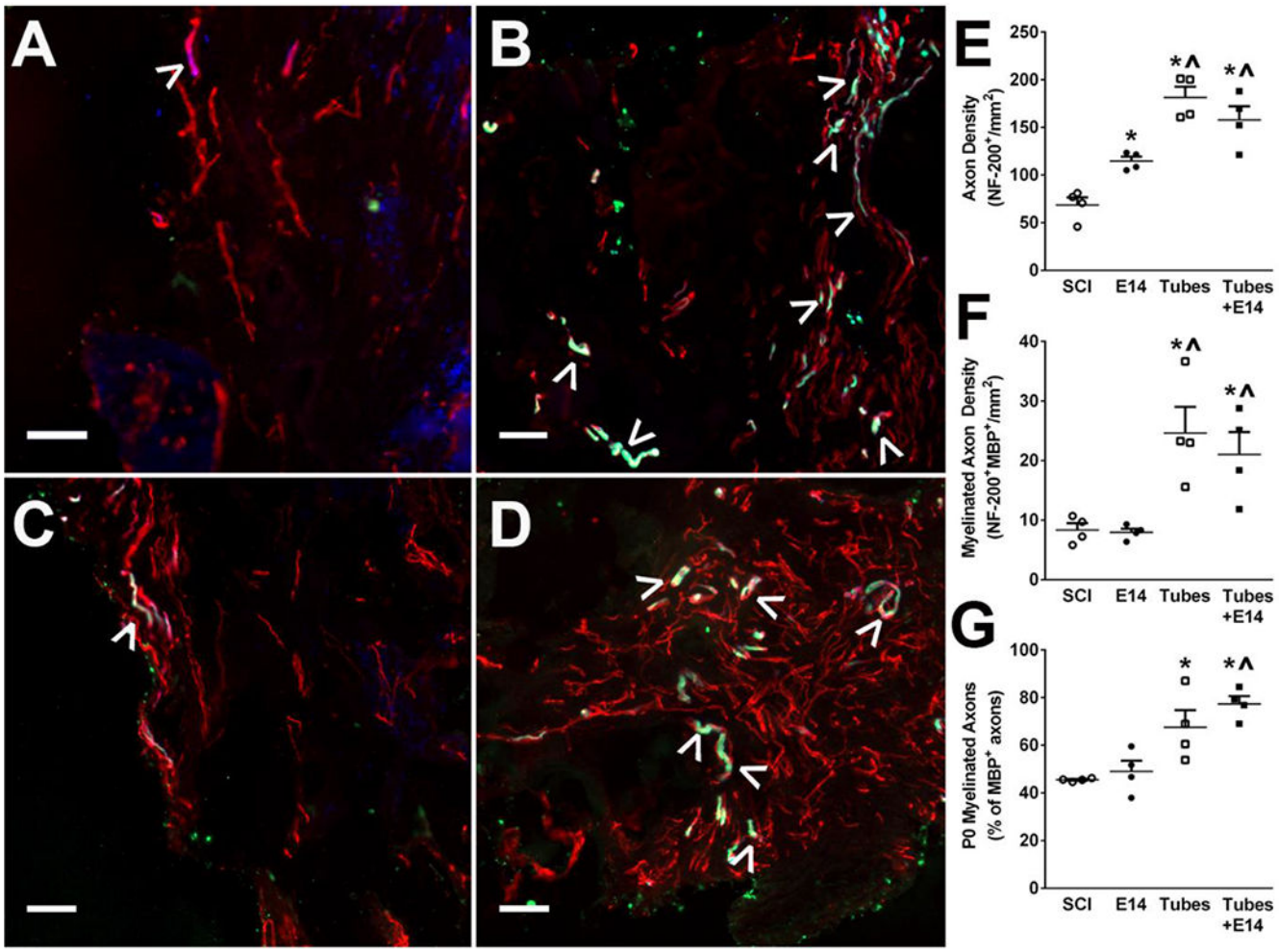

Fig. 5.

Tube implants facilitate axon formation and myelination with spinal progenitors at 4 weeks post-injury. Axon expression ($NF\text{-}200^+$, red) and myelination (MBP^+, green) is qualitatively greater in all conditions compared to SCI control (A) and E14 alone (C). Quantitatively, Tubes alone (B) and Tubes+E14 (D) had a significant increase in axon density (E) and myelinated axon (denoted by ^) density (F) over SCI and E14 only controls while E14 only had a significant increase in axon density over SCI only. Myelination source was quantified (G) with tubes and Tubes+E14 having a significantly greater number of axons myelinated from Schwann cells (MBP^+P0^+, green and blue). Data are represented as mean ± SEM. n=4 animals per condition, * $p<0.05$ (compared to SCI), ^ $p<0.05$ (compared to E14 only), 50 μm scale bars.

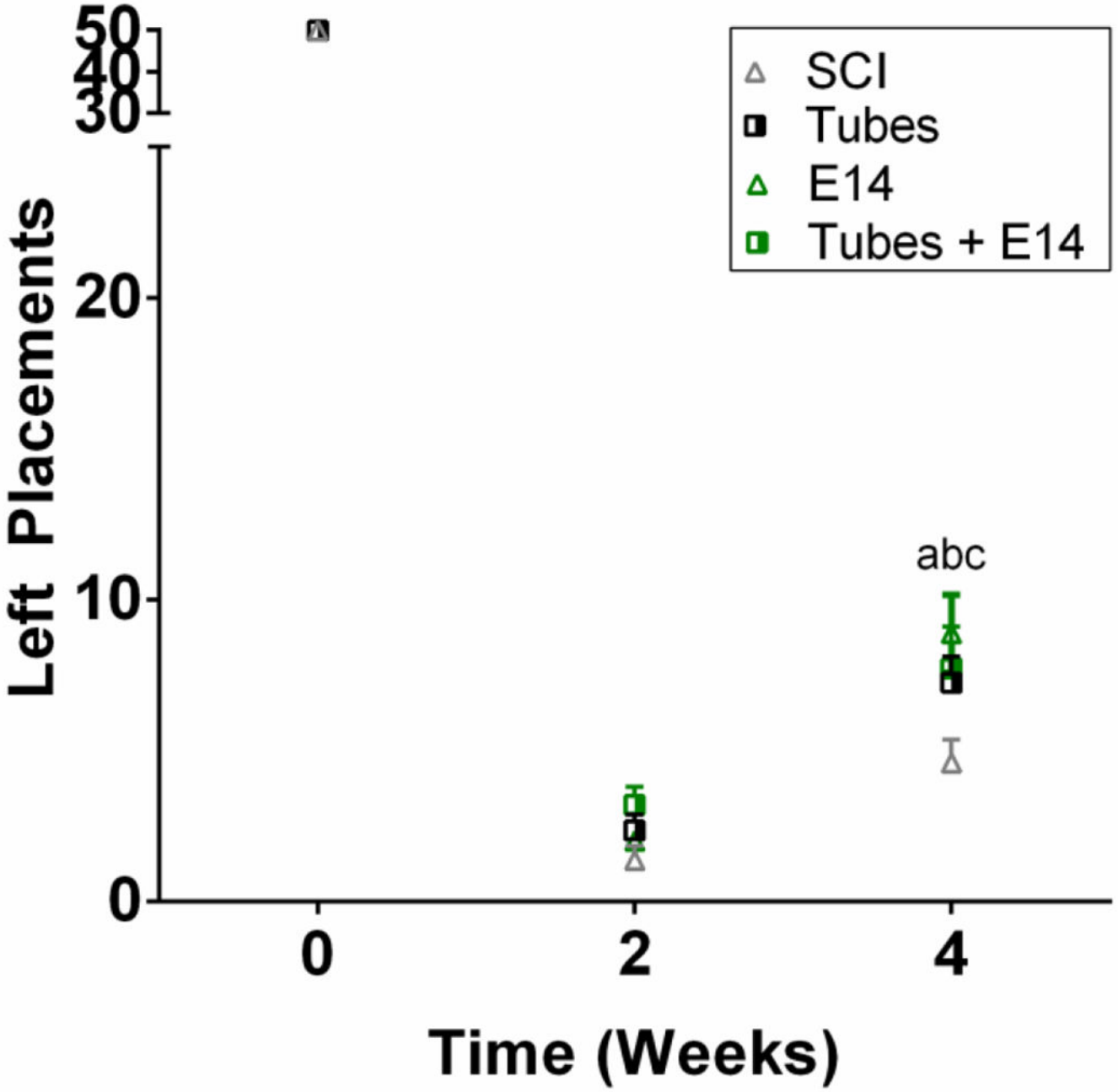

Fig. 6.

Improved forelimb stepping was observed compared to injury only controls. To assess mobility, a horizontal ladder beam test was used. Mice were trained on walking across the ladder prior to injury. Mobility was assessed through successful placements as a score out of 50 possible rungs. At 4 weeks post-injury Tubes+E14 (a, $p<0.01$), E14 alone (b, $p<0.001$), and Tubes alone (c, $p<0.05$) exhibited improved stepping compared to the injury only control. n=12 per condition.